

Control of calcium carbonate mineralisation using biopolymeric templates

DC Bassett^{1*}, B Marelli^{2§}, SN Nazhat^{1,2}, JE Barralet¹

¹Faculty of Dentistry and ²Department of Mining and Materials Engineering, McGill University, Montréal, QC, Canada. *Present address: Department of Physics, NTNU, Trondheim, Norway.

§Present address: Department of Biomedical Engineering, Tufts University, Boston, USA.

INTRODUCTION: Calcium carbonate (CaCO_3) is the most abundant biomineral that is biogenically formed with a vast array of nano and microscale features. Among the less stable polymorphs present in mineralised organisms, the most soluble, amorphous calcium carbonate (ACC), formed in chitin exoskeletons of crustacea is of particular interest since the aqueous stability of isolated ACC is limited to a few hours in the absence of polyanions or magnesium [1]. Amorphous compounds are also thought to play a significant role as precursors to crystalline phases in both invertebrate [2] and vertebrate hard tissues [3]. Here we investigated the influence of a selection of biopolymers and demineralized lobster shell on the formation and stability of calcium carbonate, and then went on to investigate the ability of this phase to act as a precursor for the synthesis of a bone-like collagen scaffold.

METHODS: CaCO_3 was precipitated in the presence of biopolymers using the NH_4CO_3 diffusion method into aqueous CaCl_2 solution in a bell jar. Samples were characterised using SEM, FTIR, XRD, TGA-DSC and MicroCT.

RESULTS: CaCO_3 mineralization was achieved in all biopolymers tested, but was particularly abundant in collagen hydrogels (Fig 1), in which a significant proportion (~18%) was found to be amorphous, as determined by FTIR and DSC measurements. In dense collagen gels, this amorphous fraction did not crystallize for up to six weeks in deionised water at room temperature. Attempts were also made to remineralize demineralised lobster shell using the same technique; although amorphous-like deposits were observed forming on the chitin matrix using SEM, ACC could not be determined using spectroscopic or calorimetric techniques.

Upon immersion in phosphate containing solutions, the calcium carbonate present within the collagen hydrogels was readily converted to carbonated hydroxyapatite, enabling the formation of a stiff bone-like composite containing 78 wt% mineral, essentially equivalent to cortical bone.

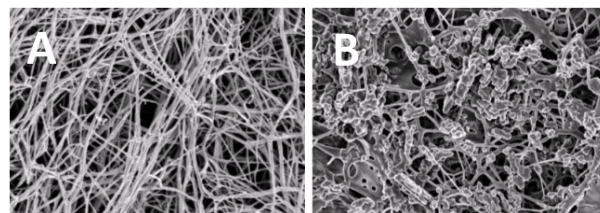


Fig 1 – SEM micrographs of as formed nanofibrillar collagen gel (A) and following mineralisation with CaCO_3 showing abundant mineral deposits throughout the hydrogel matrix (B). Frame width 10 μm .

DISCUSSION & CONCLUSIONS: The reason why collagen in particular should stabilise the ACC phase remains obscure, although our results strongly suggest that fibre diameter, fibre spacing, and the amphoteric nature of collagen fibres were critical factors. Since the initial calcium carbonate containing gels remained flexible and then stiffened on conversion to hydroxyapatite, this demonstrates the potential of this approach for the formation of readily mineralizable hard tissue scaffold materials that could be applied through minimally invasive techniques. Our work also points to the similarity in nanostructure, particularly the curvature of nanofibres present in collagen and chitin being a key factor in their ability to stabilise amorphous calcium minerals.

REFERENCES: ¹L. Glazer, A. Shechter, M. Tom, Y. Yudkovski, S. Weil, E. D. Aflalo, R. R. Pamuru, I. Khalaila, S. Bentov, A. Berman, A. Sagi, J. Biol. Chem. 2010, 285, 12831. ²H. A. Lowenstam, S. Weiner, Science 1985, 227, 51. ³a) J. Mahamid, A. Sharir, L. Addadi, S. Weiner, Proc. Natl. Acad. Sci. USA 2008, 105, 12748; b) N. J. Crane, V. Popescu, M. D. Morris, P. Steenhuis, M. A. Ignelzi, *Bone* 2006, **39**, 434; c) R. M. Biltz, E. D. Pellegrino, *Clin. Orthop. Rel. Res.* 1977, 279.

ACKNOWLEDGEMENTS: The authors acknowledge grant support of NSERC, the Quebec Ministère pour la développement économique, innovation et Exportation (MDEIE) and CFI.

Antibacterial effects of native and methacrylate modified chitosan

IS Dragland, T Knarvang, HM Kopperud

NIOM –Nordic institute of Dental Materials, Oslo, Norway

INTRODUCTION: Commercial resin-based composites are mainly composed of dimethacrylate-based monomers, such as triethyleneglycol dimethacrylate (TEGDMA), inorganic fillers and a coupling agent. Cured resin-based composites have no antibacterial effect against oral bacteria [1] and half of all fillings replaced are because of new caries [2].

Chitosan is a natural carbohydrate polymer derived from the deacetylation of chitin. Chitosan has been shown to have an inhibitor effect on the adherence of oral bacteria onto human tooth surfaces [3]. Chitosan has a polycationic carbohydrate structure with three reactive functional groups. The positive charged amino groups are suggested to be the cause of chitosan's antimicrobial activity.

Functionalization of chitosan with methacrylate groups allows for copolymerization with the resin in dental materials. This means that chitosan can be incorporated in resin-based composites in order to produce material with antibacterial activity.

The aim of the present study was to study the antibacterial effects of modified chitosan, adding functional methacrylate groups.

METHODS: Low molecular chitosan, MW 150 kDa, ca 80 % deacetylation, was modified with methacrylate groups using a method of Flores-Ramirez [4]. The product was examined for its ability to inhibit planktonic growth and formation on biofilm for Gram-positive *Staphylococcus epidermidis* and Gram-negative *Escherichia coli*.

Planktonic growth after 18 h was examined for different concentrations of chitosan in growth medium, by counting of colony forming units (CFU). Biofilm, on polystyrene or composite discs, was allowed to form, 18 h for *S. epidermidis* and 24 h for *E. coli*. Total mass of biofilms were investigated by measuring optical density (OD) at 530 nm after staining with 0.1% solution of safranin. Chitosan is insoluble in most solvents, but is soluble in dilute organic acids and all experiments were therefore done at a pH 5.9.

RESULTS: Chitosan demonstrated to inhibit planktonic growth and biofilm formation depending on the concentration of chitosan in the medium. The results of the two test models suggest that chitosan has a higher antibacterial activity against *S. epidermidis* than against *E. coli*.

Chitosan could be modified with a methacrylate functionality, but the modified chitosan had poor solubility and had low antibacterial effect compared to natural chitosan.

DISCUSSION & CONCLUSIONS: Modified chitosan was prepared and incorporated into resin-based composites during polymerization. However, no antibacterial effect on the formation of biofilm was observed. This could be explained by blocking of antibacterial amino groups during modification. The study continues with improvements of the chitosan modification.

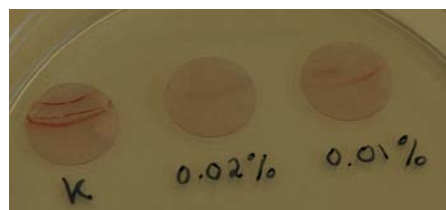


Fig. 1: Images of biofilm formed by *E. coli* on polystyrene discs. Control, K, and two different concentrations of chitosan in medium. *E. coli* form biofilm in the liquid-air interface.

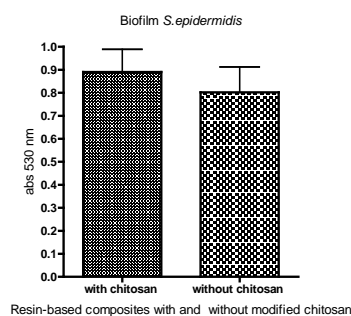


Fig. 2: OD of biofilm of *S. epidermidis* formed on composites with and without incorporation of modified chitosan.

REFERENCES: ¹ S. Imazato (2003) *Dent Mater* **19**:449-57. ² V Deligeorgi, IA Mjør, NH Wilson (2001) *Prim Dent Care* **8**:5-11. ³ H Sano, K Shibasaki, T Matsukubo et al. (2001) *Bull Tokyo Dental College* **42**:243-9. ⁴ N. Flores-Ramirez, E.A. Elizalde-Pena, S.R. Vasquez-Garcia, et al. (2005) *J Biomater Sci Polym Ed* **16**: 473-88.

ACKNOWLEDGEMENTS: Fruitful discussions with Jessica Lönn-Stensrud and Jon E Dahl are greatly appreciated.

Evaluation of silver distribution within the silver doped hydroxyapatite

A Dubnika, D Loca, D Jakovlevs, L Berzina-Cimdina

RTU Rudolfs Cimdins Riga Biomaterials Innovations and Development Centre, Riga, Latvia

INTRODUCTION: Implantation often leads to infection risks, which can result in complications and implantation failure therefore in last few decades implant materials containing antibacterial agents have been extensively studied. Silver containing materials have a very broad spectrum of antibacterial properties including ability to interact with bacteria proteins and enzymes. These materials are used for different applications and in various forms due to the antibacterial activity of silver cation (Ag^+) and other silver species like Ag^0 [1,2]. Such materials can avoid biofilm growth and prevent bacterial colonization on various surfaces. Combination of silver antibacterial properties and hydroxyapatite (HAp) bioactivity, biocompatibility and osteoconductivity leads to materials which are biocompatible and bactericidal [3]. Various researches of silver doped hydroxyapatite (HAp/Ag) synthesis and evaluation can be found, but scarce information can be found on evaluation of silver distribution within powders and pallets depending on the material preparation method. Silver distribution is essential parameter responsible for silver release and material *in vitro* properties.

METHODS: HAp/Ag was prepared, using two modified wet chemical methods: A) from calcium oxide and phosphoric acid and B) from calcium nitrate, diammonium hydrogen phosphate and ammonia solution. For both methods silver nitrate was used as a source of silver. Dried precipitate was milled to obtain fine powder. Before sintering powders were uniaxially pressed into pallets. Samples were sintered in temperature range from 500°C to 1150°C . Porosity, shrinkage, surface area, surface morphology and silver distribution within the prepared pallets after sintering were evaluated.

RESULTS: Dried and milled HAp/Ag particles prepared with method A are rounded before sintering, but HAp/Ag particles prepared with method B are needle shaped (Fig.1.). Increasing sintering temperature, particles tend to agglomerate in larger clusters and the crystallinity of the material increases. Results of BET surface area measurements are summarized in table 1. It was found that it is possible to prepare nanoscale HAp/Ag particles by using method B.

Silver distribution within the pallets indicated that silver concentration decreases on the pallet surface by increasing the sintering temperature. HAp/Ag samples prepared using method B showed increased stability towards the sintering temperature.

Table 1. Silver amount and BET surface areameasurements

	Theoretical silver amount, wt%	Incorporated silver amount, wt%	BET Surface Area, m^2/g
HAp/Ag (A)	0,30	0,27	55,95
HAp/Ag (A)	2,00	1,92	58,42
HAp/Ag (B)	0,30	0,29	49,63
HAp/Ag (B)	2,00	0,45	79,83

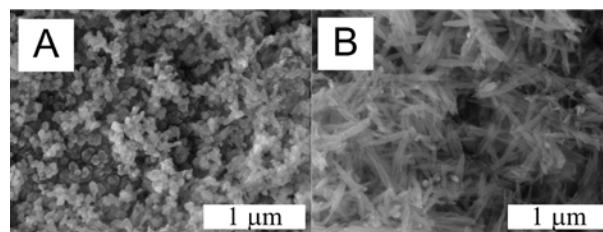


Fig. 1: Images of HAp/Ag particles, A – prepared by method A; B – prepared by method B

DISCUSSION & CONCLUSIONS: During sintering, at first, silver recrystallizes on the surface of HAp particles and increasing the sintering temperature it evaporates from the surface. Silver distribution within the pallets indicated that silver concentration within the pallets and on the pallet surface depends on the sintering temperature.

REFERENCES: ¹J. Suwanprateeb, F. Thammarakcharoen, K. Wasoontarat, et al (2012) *J Mater Sci: Mater Med* **23**: 2091-100. ²S. Nath, S. Kalmodia, B. Basu (2010) *J Mater Sci: Mater Med* **21**: 1273-87. ³X. Bai, K. More, C.M. Rouleau, et al (2010) *Acta Biomater.* **6**: 2264-73.

ACKNOWLEDGEMENTS: This work has been supported by the European Social Fund within the project “Support for the implementation of doctoral studies at Riga Technical University”.

Evaluation of the wireless measurement protocol to study the water penetration into the degradable polymers.

V Ellä^{1*}, T Salpavaara^{2*}, M Rinkkala¹, S Khan¹, J Lekkala², M Kellomäki¹

¹ Department of Biomedical Engineering Tampere University of Technology, Finland ² Department of Automation Science Engineering, Tampere University of Technology, Finland (*equal contribution)

INTRODUCTION: The passive resonance sensors are LC circuits which are measured via inductive coupling between the sensor and the reader coil. The measurand affects the resonance frequency of the circuit due to the inductance or capacitance. The geometry of the LC-circuit affects the sensitivity of the circuit. It is prone to environmental effects due to the parasitic components, mainly the parasitic capacitances [1]. This phenomenon was evaluated in regards to the water intake properties of biodegradable polymers.

METHODS: The study included embedding of resonance sensors and manufacturing of polymer rods. The resonance coils were made as described in [1]. The circuits were encapsulated between the compression moulded sheets of both polycaprolactone (PCL) homopolymer and PLCL (70/30 L-lactide/caprolactone) copolymer (Purac Biochem bv, the Netherlands). The samples were round (diameter of 22 mm) with thicknesses of 2.40 mm (PCL) and 2.09 mm (PLCL). The round polymer rods (thickness of ~10 mm) were extruded from the same polymer granules using a twin screw extruder. The rods were cut to ~20 mm pieces. Both the encapsulated circuits and the polymer rods were incubated in "Sörensen" phosphate buffer solution for 16 days, in 37°C.

RESULTS: The shift of resonance frequency of the sensor (corresponding phase maximum shift of the impedance measurement) is plotted in Fig 1. After the initial drop, the resonance shifts into lower frequencies with the PLCL polymer, whereas with the PCL polymer the resonance frequency is decreasing steadily until the day 4 after which the decrease slows down. The weight increase of the PCL reached its maximum also at day 4, while the weight of the PLCL rods increased steadily throughout the measuring time.

DISCUSSION & CONCLUSIONS: For the first time, the embedded resonance circuit measurement to estimate the changes in biodegradable polymer properties was evaluated. Changes in electrical properties were comparable to the measured weight gain of polymers.

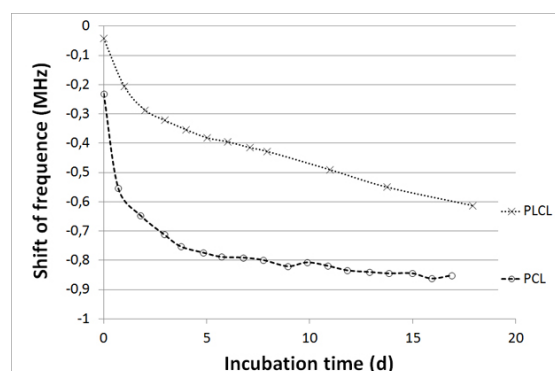


Fig. 1. The shifts of phase maxima of the resonance circuits.

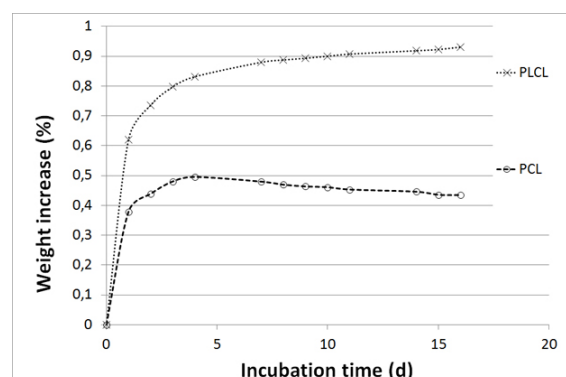


Fig. 2. Weight increase of the polymers.

The phase shift of the measured impedance curve can be used to estimate the material properties as the shape of the curve changes after the water penetrates into the polymer structure. The rate of water penetration into the polymer can thus be assessed using this method. More polymers with different properties and different layer thicknesses should be studied. To identify the actual water penetration into different layer thicknesses can give more information on the degradation dynamics.

REFERENCES: ¹ T. Salpavaara, J. Lekkala, S. Khan, et al. (2012) Proc. of the 2012 IEEE, 12th Int. Conf. on BioInformatics & BioEngineering (BIBE), Nov. 11-13, 2012, Larnaca, Cyprus IEEE, pp. 323-327.

In situ monitoring live cell populations within degradable 3D matrices

A. Finne-Wistrand¹

¹*[KTH Fibre and Polymer Technology](#), Chemical Science and Engineering, KTH Royal Institute of Technology, Sweden*

INTRODUCTION: The majority of cell culture studies have been performed using 2D substrates such as micro well plates, tissue culture flasks, and Petri dishes because of the ease, convenience, and high cell viability of the 2D culture. While conventional 2D cell culture systems have improved the understanding of basic cell biology, it has been found that 2D culture systems do not allow full exploration of the interactions between the cells of bone marrow. In this context, 3D highly porous scaffolds have been formed and a novel lab-on-a-chip based semi-high throughput system developed to observe scaffold-cell interaction in tissue engineering. Using the latest innovations in microfabrication technology, 3D microfluidic cell culture systems have been used as an attractive alternative to traditional 2D culturing systems as a model for long-term microscale cell-based research.

METHODS: A microfluidic device was designed and fabricated using a standard soft lithographic technique. A porous poly(LLA-b-TMC) matrix was introduced into the flow channel of the PDMS-chips through a solvent-casting-particulate-leaching technique, Fig. 1.



Fig. 1: Schematic cross-section of the microfluidic device

Confocal microscopy was used to monitor the cells, the single cells were followed by repeatedly observing one predetermined location in the channel.

RESULTS: The way of producing 3D scaffolds are crucial since it influence the pore morphology and thereby the cell-material interactions. The pores from particulate-leaching, phase separation and 3D fiber deposition is compared in Fig. 2. The differences are apparent.

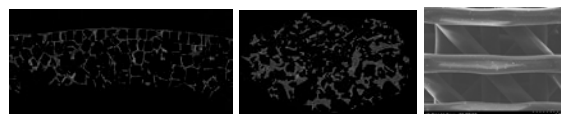


Fig. 2: Left: solvent casting, Middle: phase separation, Right: 3D fiber deposition

To evaluate, at single-cell level, the differences between different scaffolds and adapt cell-material interactions, we developed a novel microfluidic device for long-term high resolution *in situ* imaging.¹ The device was designed to permit repeated high-resolution fluorescent imaging of the same live cell populations within the 3D structure. The system were first evaluated by culturing periodontal ligament cells in the microchannel and repeatedly stained in a fluorescence-based live/dead-assay. The same cell was followed and the survival and proliferation was good during five weeks. In addition, extracellular calcium deposits were formed. Channels were stained with xylenol orange at different times and after 35 days in culture, quantifiable calcium deposits were detectable.

DISCUSSION & CONCLUSIONS: A device where we gain detailed information about the material-cell interaction has been developed and evaluated. The benefit of the system is that it is possible to track cell development at the same spatial location throughout several weeks. In addition, it is possible to follow the production of extra cellular matrix. This simple and versatile device should be readily applicable for evaluating cell-material interaction by long-term culture and high-resolution bioimaging.

REFERENCES: ¹ S. Dånmark, M. Gladnikoff, T. Frisk, et al (2012) *Biomed. Microdevices* **14**:885-93 ²T. Tyson, A. Finne-Wistrand, A-C. Albertsson (2009) *Biomacromolecules* **10**:149-54 ³S. Dånmark, A. Finne-Wistrand, M. Wendel et al (2010) *J. Bioact. Compat. Polym.* **25**:207-23

ACKNOWLEDGEMENTS: The author acknowledges KTH Royal Institute of Technology for financial support and Dr Aman Russom (KTH Royal Institute of Technology) and Prof. Kamal Mustafa (University of Bergen) for the collaboration throughout this project.

Electro-coating of titanium-zirconium and titanium with enamel matrix derivate showed enhanced in-vitro performance

MJ Frank¹, MS Walter¹, M Rubert², B Thiede³, M Monjo^{1,2}, J Reseland¹, [HJ Haugen](#)¹,

and SP Lyngstadaas¹

¹[Department of Biomaterials](#), Faculty of Dentistry, University of Oslo, Oslo, Norway. ²Department of Fundamental Biology and Health Sciences, University of Balearic Islands, Palma de Mallorca, Spain. ³The Biotechnology Centre of Oslo, University of Oslo, Norway.

INTRODUCTION: Titanium based implants have shown good clinical success over the recent years. In the quest of further improving the biocompatibility of implant surfaces, biochemical modification of the surface has been an area of keen interest over the recent years [5]. Lyngstadaas and Ellingsen suggested to use a polarization process to attach charged biomolecules to the surface in order to stimulate bone healing [4]. Promising results of enamel matrix derivate (EMD) supporting periodontal bone regeneration and the angiogenic effect of EMD have been shown [1]. The present study aimed at coating titanium based surfaces with EMD by cathodic polarization.

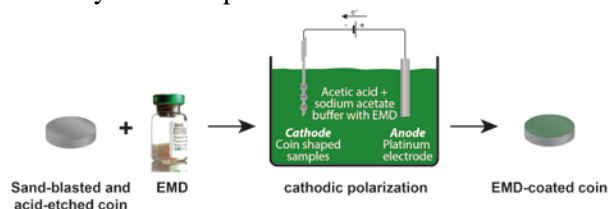


Fig.1: EMD-coating procedure.

METHODS: This study used coins made from Ti and TiZr with a sand-blasted and acid-etched surface (SBAE), as they have been described in our previous study [2]. Samples were electro-coated with EMD by a cathodic polarization process in an acetic buffer solution (Fig.1). Coated surfaces were assessed by SIMS, XPS, SEM, and MALDI-TOF MS. A cell study on EMD-coated coins was done with MC3T3-E1 cells.

RESULTS:

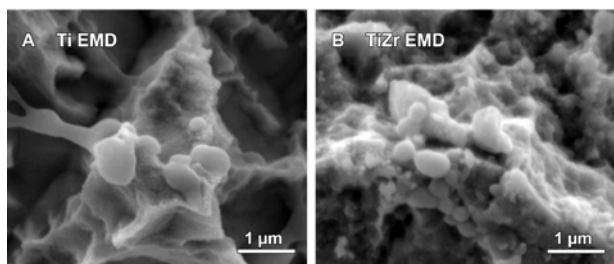


Fig.2: SEM images revealed EMD on the surface after coating.

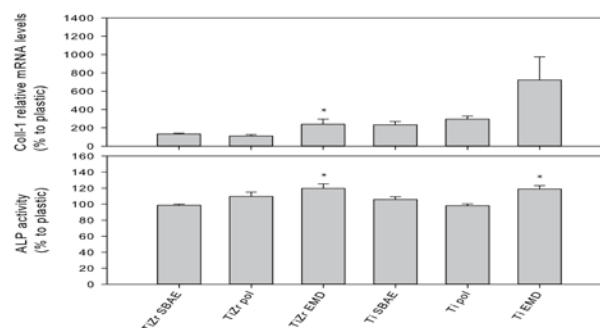


Fig.2: Results of the cell study.

DISCUSSION & CONCLUSIONS: Successful coating of the surface with EMD by cathodic polarization (Fig.1) has been proven by chemical analysis of TiZr EMD and Ti EMD by SIMS and XPS. Both materials showed increased carbon, organically bond oxygen, and nitrogen levels on the surface that were corresponding to EMD. The masking of the base material observed in XPS supported the conclusion of a successful surface coating. SEM images (Fig.2) showed nano-spheres and nano-rods on the surfaces of both materials that could be identified to be EMD [3]. MALDI-TOF MS analysis of EMD coated samples showed mass peaks corresponding to EMD [6]. The results of the cell study (Fig.3) showed an improved performance of TiZr EMD and Ti EMD when compared to the respective SBAE surfaces.

REFERENCES: ¹Cattaneo V et al., J Per Res 2003 38(6):568-574. ²Frank MJ et al., Mater Sci Eng C 2012 in press, 10.1016/j.msec.2012.12.027 ³Gestrelius S et al., J Clin Periodontol 1997 24(9):678-684. ⁴Lyngstadaas SP et al. patent WO/2002/045,764. 2002. ⁵Morra M et al., Eur Cell Mater 2006 12(1-15). ⁶Riksen EA et al., Eur J Oral Sci 2011 119(357-365).

ACKNOWLEDGEMENTS: This work was supported by the Norwegian Research Council (Grant 203034). Research materials were kindly provided by Institut Straumann AG, Basel, Switzerland.

Primary human gingival fibroblast response to titanium and titanium-zirconium modified surfaces

M Gómez-Florit¹, JM Ramis¹, R Xing², S Taxt-Lamolle², HJ Haugen², SP Lyngstadaas², M Monjo¹
¹*Department of Fundamental Biology and Health Sciences. Research Institute on Health Sciences (IUNICS), University of Balearic Islands, Palma de Mallorca, Spain.* ²*Department of Biomaterials, Institute for Clinical Dentistry, University of Oslo, Oslo, Norway.*

INTRODUCTION: Primary human gingival fibroblasts (HGF) represent an appropriate cell model for screening abutment surfaces that are designed to improve soft tissue integration and reduce implant failure. The aim of the present study was to evaluate the biological response of HGF to Ti and TiZr polished (P), machined (M), and machined + acid-etched surfaces (modMA), respectively.

METHODS: HGF were cultured on the different surfaces. Initial cell morphology (cytoskeleton and nuclei staining and scanning electron microscopy) and attachment (DNA quantification) were assessed. Then, the expression of several fibroblastic differentiation markers was analysed by real-time RT-PCR using SYBR green detection.

RESULTS: Cell number decreased in modMA Ti and TiZr surfaces, as seen with cell staining. HGF cultured on M and P surfaces were spindle-shaped and elongated, they grew aligned along the microgrooves on M surfaces but no clear orientation was seen on P surfaces. SEM images corroborated these findings.

Comparing Ti with TiZr, integrin- β 3 (ITGB3) expression increased in all TiZr surfaces (4-fold on average). Besides, M TiZr performed similar to M Ti, while on P TiZr several genes were upregulated compared with P Ti surfaces.

Compared with M Ti: (1) collagen-I α 1 (COL1A1), collagen-III α 1 (COL3A1), collagen-XII α 1 (COL12A1) and versican (VCAN) expression significantly decreased in both Ti and TiZr modMA surfaces, while matrix metalloproteinase-1 (MMP1) and integrin- α 2 (ITGA2) expression increased on modMA Ti/TiZr surfaces; (2) gene expression on P TiZr increased (40 % on average), while on P Ti decreased (10 % on average); (3) COL1A1 and COL12A1 expression decreased in P Ti; (4) interleukin-6 (IL6) and MMP1 expression increased on both Ti and TiZr polished surfaces (though it was only significant for IL6 in P TiZr).

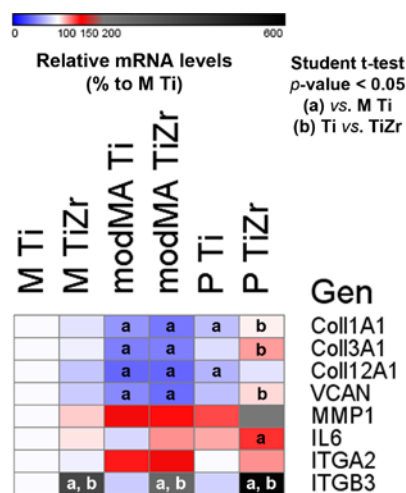


Fig. 1: Gene expression of HGF cultured on Ti/TiZr. Data represent fold changes of target genes normalized to beta-actin and GAPDH (reference genes) expressed relative to cells grown on M Ti that were set at 100 %.

DISCUSSION & CONCLUSIONS: All different TiZr surfaces showed higher ITGB3 mRNA levels compared to Ti. M surfaces did not increase MMP1 and IL6 expression, thus, showing better performance than the other studied surfaces. Taking into account the better mechanical properties and bioactivity of TiZr compared to Ti [1], the results of the present *in vitro* study show that TiZr is a potential clinical candidate for soft tissue integration and implant success.

REFERENCES: ¹Ho WF, Chen WK, Wu SC, Hsu HC (2008) *J Mater Sci Mater Med* **19**: 3179-3186.

ACKNOWLEDGEMENTS: This work was supported by the Ministerio de Ciencia e Innovación del Gobierno de España (Torres Quevedo contract to MG and JMR, and Ramón y Cajal contract to MM). Titanium and titanium-zirconium coins were kindly provided by Institut Straumann AG (Basel, Switzerland).

Scaffold materials for osteoblast engineering: Guidance from microRNA signatures and bioinformatics

JO Gordeladze¹, JE Reseland²

¹*Institute of Basic Medical Science, Department of Biochemistry, University of Oslo, Norway*

²*Institute of Clinical Dentistry, Department of Biomaterials, University of Oslo, Norway*

INTRODUCTION: Engineered osteoblasts are characterized by osteoblast specific marker genes (e.g. transcription factors, components of the BMP- and Wnt-signalling pathways), matrix proteins (e.g. collagens, osteopontin, osteomodulin), enzymes (e.g. ALP, metalloproteinases) and other markers like osteocalcin.

Bone tissue harbour many functional cell types (i.e. osteoblasts, osteocytes and osteoclasts), and bone modelling and remodelling require osteoblasts acquiring defined characteristics throughout their life span (e.g. synthesis and secretion of the osteoclast activator RANK-L and the decoy receptor OPG. For the remodelling cycle to take place, it is vital that deposited growth factors (e.g. TGFs) are released by resorbing osteoclasts to attract osteoblast to form and mineralize matrix proteins in the resorption pits. Furthermore, interplay with the immune system is necessary for proper bone maintenance. Functional bone is also dependent upon vascularization, as well as intermittent mechanical stimulation.

All these aspects are indigenous of living bone; however, engineered osteoblasts used for bone replacements hold no guarantee that proper 3D bone development and turnover will be achieved. Furthermore, mechanical stimulation may be lost or introduced too late, and the 3D structure of the engineered bone may not allow proper invasion of adjacent cell from the host. The injury, which have destroyed bone tissue in the host, may be hard to “eradicate” (e.g. cancer, chronic inflammation), thus placing a stronger demand for phenotype “resilience” on the engineered osteoblasts.

The big question then is: what would be a minimal array of growth conditions and manipulations to perform in order to stabilize engineered osteoblasts, when introduced into a defined site of injury, will develop into a proper, stable and self-renewing bone tissue?

METHODS: Despite the complexity of the proposed screening system, it may be wise to follow a given procedure, which is described briefly as follows:

1) Check different sources of stem cells for surface antigens (they should be positive for CD44, CD49, CD29, CD90, CD105 and CD106, and negative for STRO-1, CD34, CD45, and CD117), and ability to mineralize in vitro and in vivo.

2) Use selected stem cell sources and perform permutations of incubation conditions for 4-6 weeks focussing on: growth factors (TGFs/BMPs), mechanical stimulation, manipulations (through vectors with inducible promoters) of genes like transcription factors, osteoblast signature microRNAs, histone deacetylases (HDACs and Sirtuins) and various types of scaffolds.

3) Analyse gene expression profiles, focusing on a minimal size transcriptome (some 400-500 genes) encompassing genes including as many as possible of the two gene ontology terms: skeletogenesis (181 genes) and angiogenesis (172 genes), of the [Panther algorithm](#).

4) Apply the [Mir@nt@n algorithm](#) to emulate an integrated, hierarchical, regulatory loop system encompassing microRNAs, HDACs and transcripts from the osteoblast transcriptome.

5) Finally, if p-values for the GO-terms (skeletogenesis and angiogenesis) yield significantly higher probabilities for compliance with both phenotypes upon a specific permutation in stem cell differentiation (see #2 above), then one might conclude that the in vitro differentiation scheme yields useful engineered osteoblasts to be tested in vitro.

6) Use animal models with induced bone lesions to test engineered osteoblasts, and analyse for bone quality (microCT and bone strength). If deemed necessary, also check for ingrowth of vessels and the presence of attracted osteoclasts (Q-PCR of osteoclast-specific transcripts) from adjacent bone tissue.

CONCLUSIONS: In summary, this procedure of osteoblast engineering offers a way of assessing whether in vivo bone replacement (or de novo formed 3D bone tissue) will be functional and resilient to destruction over time, and thus possibly represents a guide to a more successful healing of bone lesions through osteoblast engineering from stem cells.

Does nanostructure, crystal alignment or topography affect osteoclast response?

Karlis A Gross^{1,2*}, Dirk Muller², Helen Lucas³, David Haynes³

¹*Institute of Biomaterials and Biomechanics, Riga Technical University, Latvia* ²*Dept of Materials Engineering, Monash University, Australia* ³*Dept of Pathology, University of Adelaide, Australia*

INTRODUCTION: Regenerative medicine relies on the use of resorbable biomaterials that also elicit a desired cell response; a cue for tissue growth. Previous studies have not addressed the collective effect of hydroxyapatite nanostructure, crystal alignment and topography on cell response. This work sets out to change the process parameters so that conditions are produced for a crystal alignment, and control of topography. While other processes require a post-processing stage to create topographical features on the surface, the additive feature of thermal spray processing can provide in-situ topographical refinement by the control of droplet deposition. This work will investigate the parameters that influence the generation of a topography and then investigate the osteoclast response. A comparison with dentine and a polished hydroxyapatite will show the importance of topography for the osteoclast response.

METHODS: Spray dried hydroxyapatite powder from CAM Bioceramics was sieved to 20-40 μm and flame sprayed to completely melt the powder and deposit the droplets onto a titanium surface at different preheating temperatures and spray distances. Splats were observed with a scanning electron microscope (SEM) and characterized with x-ray diffraction and Raman spectroscopy. Mononuclear cells were isolated from human buffy coats acquired from the Australian Red Cross Blood Service, and seeded onto dentine, sintered hydroxyapatite, an as-sprayed coating with topography and the same coating polished to remove the topography. Monocytes differentiated into functional OCs over 14 days, cultured in α -MEM. After 14 days, the cells were removed. Resorption pits were examined and counted by SEM. The shape was determined with a confocal microscope to determine the similarity with those found on dentine.

RESULTS: The surface temperature played an important role to avoid droplet splashing. A surface temperature of 200°C produced well-formed splats on the coating surface (Fig 1). X-ray diffraction showed a texture corresponding to c-axis alignment perpendicular to the substrate

surface. This effectively produced flattened droplets that through rapid solidification produced nanosized columnar grains throughout each splat. The resorption pits on sintered hydroxyapatite showed a small shallow dissolved section compared to the scallop shaped resorption pits on dentine. Thermal sprayed coatings showed deeper resorption than sintered hydroxyapatite, but not as uniform as dentine. The population of resorption pits was very low on sintered hydroxyapatite, however the as-sprayed coating showed a similar number to dentine. After polishing, the resorption pit population showed a 10-fold lower population.

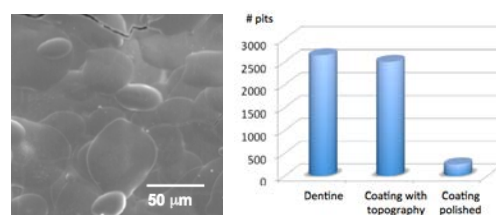


Fig. 1: The topography of the coating, and number of osteoclast resorption pits on dentine, the coating with topography and a polished coating surface.

DISCUSSION & CONCLUSIONS: The comparison of a polished coating with an as-sprayed coating showed the pronounced effect attributed to the flattened droplet topography on the coating surface. This shows the marked effect of rounded disc-like features compared to the nanosized columnar grains with a specific orientation. The splat shape may have some common topographical features to cells in the bone cell line. Surface topography created by solidified flattened droplets offers a new feature for surface design that could be applied to other types of implants. The effect of different particle sizes on splat formation has been investigated, but the influence of splat size and height on cell response requires a deeper investigation.

REFERENCES: ¹Gross et al (2012) *Acta Biomater* 8: 1948-56.

ACKNOWLEDGEMENTS: The authors are grateful for support from the Australian Research Council (Discovery grant DP0774251) and a Marie Curie grant #PIRG05-GA-2009-249306.

Biomimetic morphogenesis of calcium phosphates for biological applications

W He¹, Y Fu¹, CS Knee¹, J Bielecki², PPC de Souza³, H Schwartz-Filho³, R Jimbo⁴, M Andersson¹

¹ Department of Chemical and Biological Engineering, ² Department of Applied Physics, Chalmers University of Technology, Sweden. ³ Department of Physiology and Pathology, ⁴ Department of Oral Diagnosis and Surgery, School of Dentistry, Sao Paulo State University, Brazil. ⁵ Department of Prosthodontics, Faculty of Odontology, Malmö University, Sweden.

INTRODUCTION: Bone mineral, possessing well-defined composition and morphology, deposits within self-assembled collagen matrix. To mimic the confined space provided by collagen matrix, we use surfactant Pluronics to form liquid crystalline (LC) phases with nanometric water domains, for the study of CaP morphogenesis under spatial restriction. In addition, the crystallization of as-formed amorphous CaP (ACP) was studied via a controllable aging route and bone-like apatite was synthesized [1]. For a better understanding of the influence of surface physicochemical properties on osteogenesis, we use as-prepared CaPs to create variations in chemical composition, crystallinity and nanotopography on titanium substrates and their biological response were evaluated respectively *in vitro* cell culture and *in vivo* in a rabbit model [2].

METHODS: All chemicals were purchased from Aldrich. For synthesis using LC, Ca(NO₃)₂·4H₂O, 85% H₃PO₄ (with a Ca/P ratio of 1.67) were dissolved in Milli-Q H₂O. Then by mixing the salt solution with the surfactant (Pluronic L64 or F127) and oil, a reverse hexagonal (H₂) LC phase (15wt% salt solution, 70wt% L64 and 15wt% p-xylene), a lamellar (L_α) phase (35wt% salt solution, 55wt% L64 and 10wt% p-xylene) and a normal hexagonal (H₁) (24wt% salt solution, 60wt% F127 and 16wt% butanol) LC were formed. The LC phases were placed in an ammonia atmosphere (ammonium hydroxide, 35wt%) to start the reaction within the water domains. After 24, 72 and 96h, the reaction was stopped and the gel layer was collected according to pH and washed repeatedly using Milli-Q water and ethanol, then freeze-dried. For CaP crystallization, as-prepared ACP powders were dispersed in Milli-Q water and aged at room temperature for different times. Then the particles were purified and dried as described above. For *in vitro* and *in vivo* studies, commercially pure titanium discs (grade IV; 15.0×1.0mm) and titanium implants (3.5×7mm, Neodent Curitiba, Brazil) were spin-coated (6000 rpm, SPIN150-NPP™ spin coater, SPS-Europe BV, the Netherlands) with the ethanol dispersions

(300μL) of as-synthesized ACP and bone-like apatite nanoparticles, respectively.

RESULTS: Figure 1 shows CaPs with different morphologies synthesized from the H₂, L_α and H₁ LC phases. The spherical ACPs prepared from H₂ LC were shown to gradually convert to crystalline apatite in Milli-Q water in a controlled manner [1]. As-formed apatites with elongated morphologies (1.5–4nm wide) and specific surface area exceeding 350m²/g, presented bone-resembling features [1]. Quantitative real time polymerase chain reaction (qPCR) data shown that as-prepared bone-like apatite nanoparticles induced significantly higher up-regulation of osteospecific gene markers such as Colla1 and Spp1, as compared to using ACP as coating material [2].

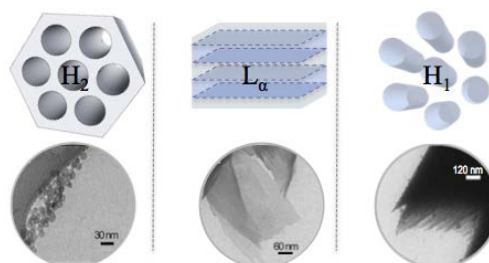


Fig. 1: CaP particles formed from LC phases.

DISCUSSION & CONCLUSIONS: Within the confined space offered by the LC phases, CaPs with different morphologies (sphere, wire, sheet, and hierarchical structures) were formed. Furthermore, the conversion of ACP to crystalline apatite in aqueous media was observed and nanocrystalline apatite with ultrahigh SSA and bone-resembling features were prepared [1]. Gene expression of cultured osteoblasts exhibited great dependence on as-formed CaP coatings [2].

REFERENCES: ¹ W. He, P. Kjellin, F. Currie, et al (2012) *Chem Mater* **24**:892-902. ² W. He, M. Andersson, P.PC de Souza, et al. Osteogenesis-inducing nanoparticle precursors applied to titanium surfaces (2012) *in submission*.

ACKNOWLEDGEMENTS: The Swedish Research Council (VR) and NanoSphere centre are acknowledged for funding.

Novel chitosan scaffolds manufactured by net-shape-nonwoven technique for bone tissue engineering applications

M. Jaeger¹, M. Hild², D. Aibibu², T. Hanke¹, H. Worch¹, Ch. Cherif²

¹ Max Bergmann Center of Biomaterials, TU Dresden, Budapester Str.27, 01069 Dresden, Germany

² Institute of textile machinery and high performance material technology, TU Dresden, Hohe Str.6, 01069 Dresden, Germany

INTRODUCTION: Chitosan has been widely investigated for bone tissue engineering applications because of its biocompatibility, biodegradability, its ability to support wound healing and osteoconduction and its antimicrobial properties [1-3]. The production of filament yarns made of pure chitosan enables their utilisation in textile manufacturing techniques which provide excellent preconditions for the engineering of highly porous scaffolds with adjustable pore size distributions.

METHODS: Scaffolds made of pure chitosan-microfibers were manufactured by the novel “net-shape-nonwoven” (NSN) technique. Short fibres were processed into three-dimensionally shaped nonwoven structures with adjustable porosity and mechanical properties, respectively (fig. 1). The chitosan scaffolds were functionalised with collagen. Porosity was measured using mercury-less porosimetry, compressive deformation behaviour was investigated.

The chitosan scaffolds and collagen-functionalised chitosan scaffolds were seeded with human bone marrow stromal cells (hBMSC). Adhesion, proliferation and differentiation of the cells were determined by biochemical analysis. The distribution of the cells seeded and cultivated on the scaffolds was visualized by performing MTT- and fluorescence staining.

the scaffolds. The differentiation into osteoblasts could also be observed.

DISCUSSION & CONCLUSIONS: As a conclusion we can say that the NSN chitosan scaffolds provide proper spatial conditions for the adhesion and ingrowth of hBMSC.

REFERENCES: ¹ C. Heinemann (2008) *Novel Textile Chitosan Scaffolds Promote Spreading, Proliferation, and Differentiation of Osteoblasts*, *Biomacromolecules*, 9, 2913-2920. ² C. Heinemann (2009), *In Vitro Evaluation of Textile Chitosan Scaffolds for Tissue Engineering using Human Bone Marrow Stromal Cells*, *Biomacromolecules*, 10, 1350-1310. ³ C. Heinemann (2010) *In Vitro Osteoclastogenesis on Textile Chitosan Scaffolds*, *European Cells and Materials*, 19, 96-106.

ACKNOWLEDGEMENTS: This research project (DFG CH 174-24/1) is supported by “Deutsche Forschungsgemeinschaft”.

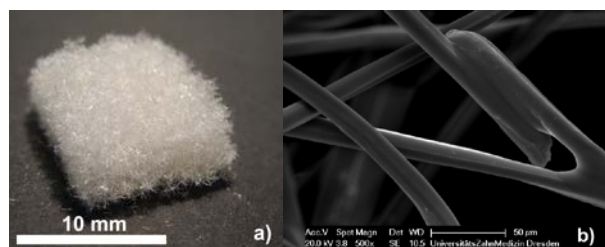


Fig. 1: Net-Shape-Nonwoven chitosan structures, complete scaffold (a); Juncture between fibers (b)

RESULTS: The NSN scaffolds showed long-time stability in various buffer salines. The porosity is a function of the fiber-length used in the scaffold. The seeded hBMSC adhered and proliferated on

Hybrid electrospun scaffold for cardiovascular tissue engineering

S Hinderer^{1,2}, D Özdemir¹, K Schenke-Layland^{1,3}

¹ [Fraunhofer Institute for Interfacial Engineering and Biotechnology \(IGB\), Stuttgart, Germany.](#)

² [Institute for Interfacial Engineering IGVT, University of Stuttgart, Germany.](#) ³ [Dept. of Thoracic and Cardiovascular Surgery and Inter-University Centre for Medical Technology Stuttgart – Tübingen \(IZST\), University Hospital, Eberhard Karls University, Tübingen, Germany](#)

INTRODUCTION: Cardiovascular disease (CVD) is worldwide the number one cause of death.¹ Currently, there is no sufficient regenerative therapy to treat CVD. Stem cell-based tissue engineering might offer viable strategies. Therefore, there is a need for the development of versatile, bio-mimicking scaffolds to improve or support cardiac function that can be easily introduced into clinics.

METHODS: Scaffold fabrication and characterization: We utilized degradable polymers that are routinely used as certified medical products. Electrospinning was performed using a customized electrospinning device. The polymers and a photo initiator were dissolved in 1,1,1,3,3,3 hexafluoro-2-propanol. The fibers were cross-linked by UV radiation. Fiber and pore sizes were analyzed by scanning electron microscopy (SEM). Furthermore, contact angle measurements and tensile testing was performed to determine hydrophilicity as well as the tensile strength and the E-modulus respectively. All data were compared to native cardiovascular tissues.

Cell-material interactions: Human vascular smooth muscle cells (hSMCs) and endothelial cells (hECs), as well as porcine valvular interstitial cells (pVICs) and valvular endothelial cells (pVECs) were seeded onto the scaffolds and characterized using routine histology and SEM. Furthermore, an MTT-assay was applied in order to determine cell vitality and cytotoxicity. To confirm phenotypes we performed immunofluorescence staining.

RESULTS: Using electrospinning, we generated a hydrophilic hybrid scaffold with an average fiber diameter of $0.37 \pm 0.08 \mu\text{m}$, which is comparable to fiber sizes seen in native cardiovascular tissues. Furthermore, the hybrid cross-linked material showed a similar morphology and tensile strength when compared to native tissues (hybrid: 3.9 ± 0.8 ; native tissue: 4.3 ± 1.0 ; $p > 0.05$). In contrast, the E-modulus differed significantly (hybrid: 177.1 ± 41.2 ; native tissue: 62.4 ± 36.7 ; $p < 0.05$). Vital and proliferating hSMCs, hECs, pVICs and pVECs adhered on the porous scaffold (**Fig. 1**).

Immunofluorescence staining confirmed that the phenotypes of the *in vitro*-cultured cells were maintained.

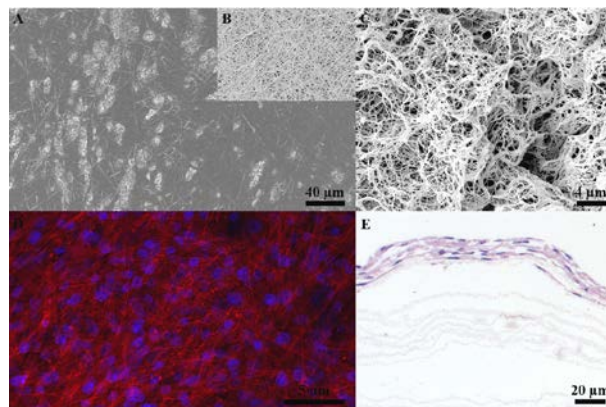


Fig. 1: A) SEM of hSMCs on an electrospun hybrid scaffold. B) SEM of the electrospun scaffold without cells. C) SEM of decellularized native cardiovascular tissue. D) Actin (red) staining of hSMCs cultured on hybrid scaffolds. Cell nuclei are blue (DAPI). E) H&E staining of hSMCs on the hybrid matrix.

DISCUSSION & CONCLUSIONS: The mechanical properties of the electrospun hybrid scaffolds are close to those seen in native cardiovascular tissue. Additionally, the developed material demonstrated excellent cell-matrix interactions, without any cytotoxic effects. Our data suggests that the generated hybrid biomaterial might be a promising tool for cardiovascular regenerative medicine.

REFERENCES:

¹<http://www.who.int/mediacentre/factsheets/fs317/en/index.html>, 11.12.2012

ACKNOWLEDGEMENTS: This study was financially supported by the Fraunhofer-Gesellschaft Internal programs (Attract 692263 to KSL), the BMBF (0316059 to KSL) and the Ministry of Science, Research and the Arts of Baden-Württemberg (33-729.55-3/214 to KSL).

In vitro cytocompatibility of *Cladophora* nanocellulose

K.Hua, D.O.Carlsson, M.Strømme, A.Mihranyan, N.Ferraz

Nanotechnology and Functional Materials, Department of Engineering Sciences, Uppsala University, Sweden

INTRODUCTION: Characterized by the exceptionally high degree of crystallinity, large surface area and broad chemical modifying capacity, *Cladophora* cellulose has a great potential as a natural biomaterial for the development of medical devices and applications in healthcare [1,2]. Nevertheless, studies are needed to confirm the safety profile of the nanocellulose material. In this study, we investigated the influence of surface charge of *Cladophora* cellulose on cell adhesion, viability and proliferation.

METHODS: *Cladophora* cellulose was modified through EPTMAC condensation and TEMPO mediated oxidation to get cationic and anionic *Cladophora* cellulose respectively. The cellulose surface charges were characterized by measuring the ζ -potential.

In vitro cytocompatibility was investigated by assessing cell adhesion and proliferation on the cellulose membranes, human dermal fibroblasts (hDF) were cultured on the surface of anionic, cationic and non-modified cellulose membranes for 24 h. Cell cultured on thermanox (TMX) served as positive control and cells cultured on TMX in the presence of 5 % DMSO were used as negative control. Cell viability was determined by the Alamar blue assay. Cell adhesion to the cellulose surfaces was studied in terms of cell number and morphology by scanning electron microscopy (SEM).

RESULTS: The ζ -potential measurements confirmed that EPTMAC condensation and TEMPO oxidation resulted in highly cationic and anionic cellulose surfaces, respectively, whereas the surface of the non-modified cellulose fibers was slightly anionic.

The Alamar blue assay showed that the cell viability was significantly higher on the anionic *Cladophora* cellulose as compared to the non-modified and the cationic cellulose.

SEM micrographs showed that a great number of fibroblasts adhered to the surface of anionic *Cladophora* cellulose membranes and showed typical fibroblast morphology. On the contrary, fewer and mainly round-shaped cells were

observed on the cationic and non-modified *Cladophora* cellulose membranes (Fig. 1).

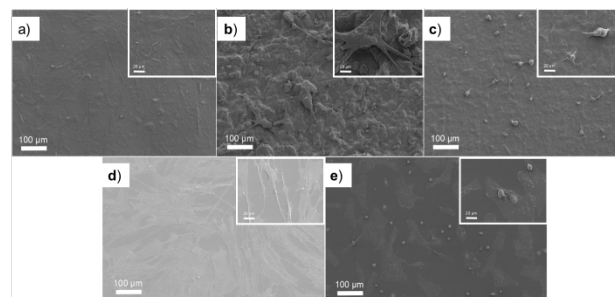


Fig. 1: SEM micrographs of hDF adhered on surfaces of non-modified a), anionic b), cationic c) *Cladophora* cellulose membranes, thermanox d) and treated with 5% DMSO e) after 24 hours culture.

DISCUSSION & CONCLUSIONS: It is likely that the different surface charges promote different patterns of protein adsorption in terms of amount, type and conformation, which in turn could affect cell adhesion and behavior. The results presented in this work suggest that anionic *Cladophora* cellulose could be a good candidate for cell culture substrate and open the possibility of its application in tissue engineering. Other material properties like specific surface area, fiber length, porosity and degree of crystallinity will be further investigated to relate such physico-chemical properties with cell behavior on the different cellulose materials.

REFERENCES: ¹A. Mihranyan (2010) *J Appl Polym Sci* **119**:2449-60. ²D. Klemm et al. (2006) *Adv Polym Sci* **205**:49-96

Comparative morphological micro-CT study of root canals in contralateral premolars

G. F. Johnsen¹, H. J. Haugen¹, S. P. Lyngstadaas¹,

¹ University of Oslo, Oslo, Norway,

INTRODUCTION: The purpose of root-canal therapy (RCT) is to treat and prevent apical periodontitis. This is accomplished by chemo-mechanical instrumentation, intra-canal placement of medicament in the case of infection, obturation of the canal with root-filling material and sealer, and, finally, a coronal restoration¹. The eventuality of micro-leakage of endodontic pathogens and their accompanying virulence factors in saliva through the seals provided by the coronal restoration and root canal filling/sealer will lead to (re)infection and failure of the endodontic treatment². The validity of models evaluating micro-leakage in endodontically treated teeth has recently been questioned with the major criticism being that the teeth/roots used are not appropriately matched, and thereby one is actually testing differences in morphology rather than differences in root filling materials³. It has been claimed that contra-lateral teeth exhibit identical morphology/anatomy, but the literature is scarce and mostly details occlusal anatomy, and, are therefore more appropriate for micro-leakage studies^{3,4}. This study's main objective is to determine the degree of similarity of contra-lateral premolars versus random pairs of premolars.

METHODS: The study has been evaluated and accepted by The National Committee for Medical and Health Research Ethics (NEM) of Norway (reference number: 2012/2092b). Contra-lateral premolars are harvested from donors undergoing orthodontic treatment at the Section of Orthodontics, Institute of Clinical Dentistry, Faculty of Dentistry, at the University of Oslo. The premolars are to be extracted for orthodontic indications. Informed and signed consent by parents/legal guardians or consenting adults is acquired prior to extraction. The tooth pairs are mechanically brushed with single-use toothbrushes in sterile saline. Organic material from root surface and cemento-enamel junction is denuded by careful curettage with periodontal curette. The teeth are stored in an ethanol humidor (70%) at constant temperature in the Department of Biomaterials' cold room. In order to determine if contralateral premolars are anatomical analogues scans are performed using the Skyscan 1172 μ CT system (SkyScan, Kontich, Belgium) and 3D

image reconstruction software (NRecon) will be done before co-registration of paired premolars, but direct comparison of morphology is not possible as the contralateral teeth are not superimposable mirror bodies, but are chiral objects (i.e. non-superimposable). SolidWorks will be used to overcome this obstacle by using the function mirror part/mirror entity prior to evaluation of similarity.⁵ A method described by Hilaga et al. called *Topology Matching* will be employed in order to match similarity between scans of contralateral premolars⁶. Statistical analysis will be done on the statistical software SPSS to determine if anatomical similarity is significant.

REFERENCES: ¹ Ørstavik, D. and T. Pitt Ford (2008), *Essential endodontology*. Oxford: Blackwell Munksgaard. ² Siqueira et al. (2007) Bacterial pathogenesis and mediators in apical periodontitis. *Brazilian dental journal*; 18:267-280. ³ De-Deus, G. (2012) Research that matters - root canal filling and leakage studies. *International endodontic journal*; 45:1063-1064. ⁴ Zehnder, M., et al. (2006) A comparative study on the disinfection potentials of bioactive glass S53P4 and calcium hydroxide in contra-lateral human premolars ex vivo. *International endodontic journal*; 39:952-958. ⁴ Archangelo, C.M., et al. (2011) Influence of buccal cusp reduction when using porcelain laminate veneers in premolars. A comparative study using 3-D finite element analysis. *Journal of prosthodontic research*; 55:221-227. ⁶ Hilaga, M., et al. (2001) Topology Matching for fully automatic similarity estimation of 3D shapes. *Comp Graph*; 203-212.

In vivo evaluation of the mechanical stability of nanopatterns applied on titanium implants by colloidal lithography

D Karazisis^{1,2}, H Agheli^{1,2}, L Emanuelsson^{1,2}, O Omar^{1,2}, J Lausmaa^{2,3}, L Rasmuson^{1,2}, P Thomsen^{1,2}, S Petronis^{2,3}

¹*Department of Biomaterials, University of Gothenburg, Gothenburg, SE.*

²*BIOMATCELL, VINN Excellence Center of Biomaterials and Cell Therapy, Gothenburg, SE.*

³*Department of Chemistry and Materials, SP Technical Research Institute of Sweden, Borås, SE.*

INTRODUCTION: Recently, increasing attention has been given to the potential role of material surface nanotopography for enhancing osseointegration. It has been shown that nanofeatures at the implant surface induce a favorable bone response¹⁻². Nevertheless, there is also a potential risk of nanoparticle detachment from the implant surface with unknown long term medical outcome. The aim of this study was therefore to investigate how the mechanical stability of the nanosurfaces produced by colloidal lithography² depends on the surface coating thickness and implantation site diameter.

METHODS: Seven machined and seven electropolished implants made of grade II titanium were used in the study. The implants were screw-shaped, 2.0 mm in diameter and 3 mm in height, with threads resembling commercially available dental implants (Fig. 1). All implants were nanopatterned topographically with colloidal lithography² using polystyrene particles of 60 nm. In order to achieve homogenous chemistry on the implant surface, a thin Ti layer of 10 nm or 30 nm was deposited by sputter coating. The implants were then installed in the medial aspect of the proximal and distal tibial metaphysis of five Sprague-Dawley rats. The insertion of the implants took place after complete removal of the lateral tibial cortical plate for selection of the inserted implants on the opposite lateral side. The implant sites were prepared with round drills of diameter 1.6 mm, 1.8 mm and 2.1 mm. The implants surface was evaluated pre- and post-insertion by scanning electron microscopy (SEM).

RESULTS: Implant insertion into the implantation site has caused detachment of nanostructures located on the outer parts of the threads. The results of implantation and SEM observations are summarized in Table 1.

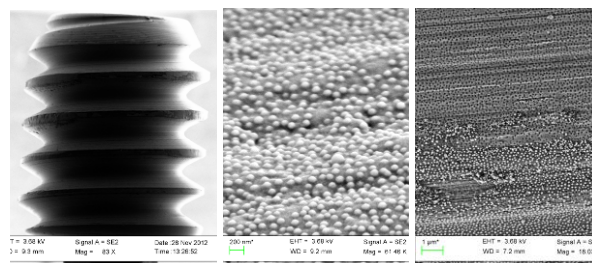


Fig. 1: SEM images of implant design (left), intact nanostructures (middle) and partly scratched off nanostructures (right).

Table 1. Implant primary stability and remaining coverage (%) of nanopattern on the implant surface after implantation

Drill diameter Implant surface type	1.6 mm	1.8 mm	2.1 mm
Polished +10nm Ti	Good, 38%	Intermediate, 75%	
Machined+10nm Ti	Good, 5%	Good, 50%	
Polished +30nm Ti	Good, 48%	Good, 85%	
Machined +30nm Ti		Good, 60%	Good, 90%

DISCUSSION & CONCLUSIONS: The study enabled selection of the optimal implantation site diameter (\varnothing 1.8 mm for electropolished and \varnothing 2.1 mm for machined implants) in terms of sufficient primary stability and minimal detachment of surface nanostructures. The higher coating thickness (30 nm versus 10 nm) improved mechanical stability of the topographical nanostructures by \sim 10%.

REFERENCES: ¹Webster TJ. Nanotechnology for the regeneration of hard and soft tissues. Singapore: World Scientific Publishers; 2007. ³Ballo A, *et al.* Nanostructured model implants for in vivo studies: influence on de novo bone formation on titanium implants. *Int J Nanomedicine*. 2011;6:3415-28.

Mesoporous Implants for Localized Controlled Drug Delivery

J Karlsson^{1,*}, N Harmankaya², A Palmquist², M Halvarsson³, P Tengvall² and M Andersson¹

¹ Dept. Chemical and Biological Engineering, Applied Chemistry, Chalmers University of Technology, Gothenburg, Sweden. ² Dept. Biomaterials, Sahlgrenska Academy at University of Gothenburg, Gothenburg, Sweden, and ³ Dept. Applied Physics, Microscopy and Microanalysis, Chalmers University of Technology, Gothenburg, Sweden

INTRODUCTION: There is an ongoing development within biomaterial technology to improve the osseointegrating performance of implants. Despite progress, further improvements are needed to achieve a more rapid healing and to enable treatment of patients suffering from low bone amounts or poor bone quality. In this study, mesoporous TiO₂ thin films were used to serve for a local drug delivery to obtain an enhanced osseointegration of implants. Two drug candidates, Alendronate (ALN) and Raloxifene (RLX), were evaluated when released locally.

METHODS: Mesoporous TiO₂ was synthesized using the evaporation induced self-assembly (EISA) method [1]. Different analytical techniques were used to characterize the mesoporous TiO₂ thin films, such as transmission electron microscopy (TEM), scanning electron microscopy (SEM), X-ray diffraction (XRD) and nitrogen adsorption. The release rate for the different drug candidates was evaluated with quartz crystal microbalance with dissipation (QCM-D). For *in vivo* evaluation removal torque (RTQ), qPCR, histomorphometry, ultrastructural interface analysis, backscattering SEM and autoradiography were used.

RESULTS: Ordered mesoporous TiO₂ thin films (200 nm thick) were successfully formed using the EISA process. The pore-width was 6 nm, with a narrow size distribution. The mesoporous TiO₂ films were deposited onto titanium implants and evaluated both *in vitro* and in three independent *in vivo* studies. An *in vitro* study showed that the pores were accessible from the implant surface and that apatite formation using SBF was higher on the mesoporous implants compared to its nonporous counterpart. An *in vivo* study in rabbits showed that mesoporous TiO₂ thin films could withstand the shearing forces during implantation into bone, and an indication that the pores increased the biomechanical interlocking was observed from RTQ measurements [2]. QCM-D was used to monitor the drug loading and release from the surfaces and it was shown that a sustained local release for both drugs, ALN and RLX, were obtained. An *in vivo* study performed in rats

demonstrated significant enhanced osseointegration for the drug containing surfaces compared to the control surfaces without drugs. In a separate rat study, the release kinetics of ALN labeled with ¹⁴C, was evaluated. The distribution of the ALN into the surrounding bone was examined using autoradiography. Data demonstrated that there was a sustained release of the radiolabeled ¹⁴C ALN, and that the released drug molecules diffused a maximum distance of about 1 mm away from the implant surface.

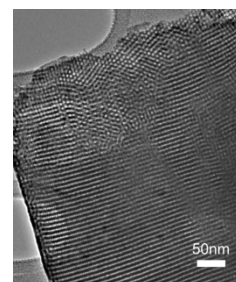


Fig. 1: An acquired TEM image of the mesoporous TiO₂ thin film.

DISCUSSION & CONCLUSIONS: Titanium implants coated with a thin mesoporous TiO₂ film can be used for local drug delivery. A sustained release was achieved both for a polar (ALN) and a non-polar (RLX) drug. It was shown *in vivo* that the films are mechanically stable and that the delivery of both drugs results in an improved osseointegration. It was shown, using TEM of the bone-implant interface, that the mesoporous also enabled bone ingrowth into the implant surface. Moreover, a release kinetic study performed *in vivo* showed that the majority of ALN remains localized to the implant surface, which is desirable to achieve an efficient treatment.

REFERENCES:

- ¹ M. Andersson et al. (2005) *Chem. Mater.* **17**: 1409-1415.
- ² J. Karlsson et al. (2012) *Acta Biomater.* **8**: 4438-4446.

ACKNOWLEDGEMENTS: The authors gratefully thank the Materials Area of Advance at Chalmers University of Technology for providing the financial support.

Ultrasonic coating technique of a polymer scaffolds for bone implant applications

A Kędzierska¹, B Ostrowska², D Smoleń¹, E Pietrzykowska¹, W Świążkowski²,
A Gedanken³, W Łojkowski¹

¹ Institute of High Pressure Physics, Polish Academy of Sciences, Poland, ² Faculty of Materials Engineering, Warsaw University of Technology, Poland, ³ Department of Chemistry, Bar Ilan University, Israel

INTRODUCTION: The idea of scaffolds for bone regeneration is to facilitate bone regrowth when the gap in it is too large for its natural healing. This can frequently happen after severe bone fractures, removal of bone tumours, craniomaxillofacial surgery, etc. Currently used bone implants are not fulfilling clinician's criteria. The bone regrowth process is too slow, the voids filling is incomplete, inflammatory processes may take place, and mechanical strength of the scaffold is low. In present work the ultrasonic technique was applied to produce a nanohydroxyapatite layer on the polymeric scaffolds surface. It is expected that the formed layer will significantly improve the cell attachment by changing the polymer surface properties, e.g. topography.

METHODS: Used hydroxyapatite nanopowder referred to as "GoHAP" was obtained by microwave solvothermal synthesis process fully described in previous publications [1, 2]. The GoHAP's solubility determined according to the ISO 10993-6:2007 procedure. Its biodegradation rate was a few times higher in comparison to commercially available HAp nanopowders [2]. Ultrasonic coating technique is simple, relatively cheap process which permits to control the coating texture, also at nano-scale approach. US technique allows to apply different kind of powders and necessary additions. In this study this technique was applied to form the GoHAP layer on the polycaprolactone scaffolds surface.

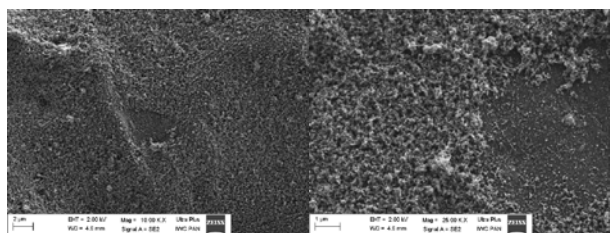


Fig. 1: The SEM micrographs of hydroxyapatite coating on scaffold surface.

The GoHAP layers formed on the polycaprolactone scaffolds were investigated by the Scanning Electron Microscopy (SEM) (Fig. 1.), Atomic Force Microscopy (AFM), Energy Dispersive Spectroscopy (EDS) in order to test the coating texture, composition and strength of ceramic-to-polymer joint. Furthermore, the wetting angle for water was determined by Sessile Drop Technique.

RESULTS: The presence of hydroxyapatite layer is causing the decrease of wetting angle compared to pure polycaprolactone surface. The thickness of the coating was measured by Atomic Force Microscopy is between few nanometers up to 350 nm for different samples.

Table 1. Wetting angle values for pure polycaprolactone surface and coated with hydroxyapatite nanoparticles.

	Pure polycaprolactone	Polycaprolactone with GoHAP layer
Wetting angle [deg]	71,8	33,7

DISCUSSION & CONCLUSIONS: The method of obtaining GoHAP layers on the polymer scaffolds surface with ultrasonic technique is a promising technology for the enhance bone regrowth process. Obtained scaffolds will be investigated by in vitro and in vivo tests.

REFERENCES: ¹ Patent application P-369906, ² Smoleń, D. et al, *J Nanomaterials* (2012), **2012**, doi:10.1155/2012/841971

ACKNOWLEDGEMENTS: This work was financed by the European Regional Development Fund in the frame of the SONOSCA (NCBiR/ERA-NET-MATERA/04/2011) and BIO-IMPLANT (POIG.01.01.02-00-022/09) as well as the use of equipment funded by the project CePT.

Viscous mass foaming – new technology for preparation of porous TCP ceramics

J Locs¹, V Zalite¹, L Berzina-Cimdina¹

¹ Riga Biomaterials Innovation and Development Centre, Riga Technical University, Riga, Latvia.

INTRODUCTION: The *in situ* viscous mass foaming with ammonium bicarbonate (NH_4HCO_3) as foaming agent was used for the preparation of porous beta tri-calcium phosphate ceramics. Current technology has been described before with application to produce porous hydroxyapatite ceramics [1-2].

METHODS: Calcium deficient powder used for porous ceramic preparation was prepared by a wet precipitation reaction between calcium hydroxide suspension (CaO, Riedel-de Haën®, Germany) and orthophosphoric acid solution (H_3PO_4 , 85%, Sigma-Aldrich, Germany). The dried precipitates were milled to obtain a fine powder. To attain a highly viscous/plastic mixture, powder was mixed with liquid phase glycerol ($\text{C}_3\text{H}_5(\text{OH})_3$; purity > 99,8%, Ltd. BIO-VENTA, Latvia). A pore forming agent in amount less than 2 % by weight were added to the mass. Prepared mass was placed in cylindrical moulds and then heated increasing temperature from 40 to 110 °C for proceeding the foaming process and particular release of organic additive from the sample. The samples were sintered at 1150 °C for 2 hours, obtaining beta tricalcium phosphate crystalline phase porous bioceramic samples. Sample dimensions were as following: 6 mm in diameter and 4 mm in height.

RESULTS: *In situ* viscous mass foaming leads to the formation of porous structure with well-connected open porosity. In current research the samples with 50 % porosity and pore size distribution from 10 to 500 µm. The average pore size was around 200 µm and pore wall thickness 100 µm. The addition of foaming agent and liquid phase, as well as gases eliminated during the foaming (CO_2 , H_2O , NH_3) do not affect the purity and phase composition of sintered ceramics.

DISCUSSION & CONCLUSIONS: The formation of open, round shaped channels is ensured by the relatively large amount of eliminated gases occurred during thermal decomposition of ammonium bicarbonate. As it can be seen in Fig. 1, the certain inhomogeneity of porosity, mainly expressed as some larger pores is created. Formation of such “giant” pores occurs due to the agglomeration of pore forming agent with following elimination of larger amount of gases. The proposed *in situ* viscous mass foaming technology is a promising technology for the

manufacturing of porous ceramics. The specific attention must be focused to the preparation process and homogeneity of the mass.

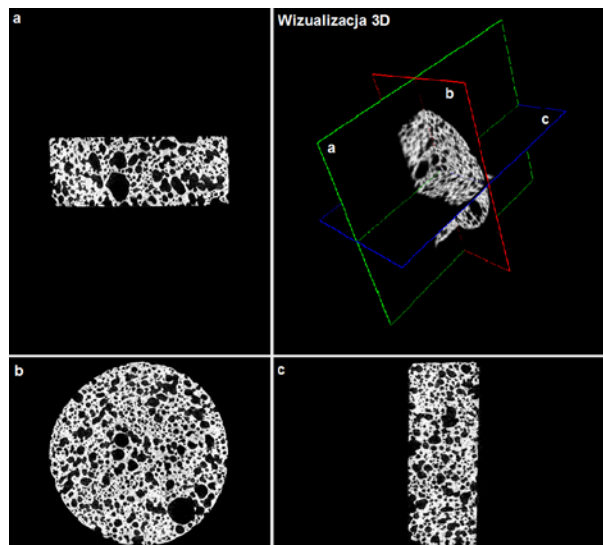


Fig. 1: Micro computed tomography images of prepared and sintered porous beta tricalcium phosphate ceramics.

REFERENCES: ¹ V. Zalite, J. Locs, D. Vempere and L. Berzina-Cimdina (2012) *Key Eng Mat* **493-494**:277-80. ² V. Zalite, J. Locs, D. Vempere and L. Berzina-Cimdina (2010) *Eur Cells Mater* **20**:280.

ACKNOWLEDGEMENTS: This work has been supported by ERA-Net MATERA/BBM-2557 project SONOSCA “Sonochemical technology for bioactive bone regeneration scaffold production”.

Immune responses to topographically different calcium phosphate cements

G. Mestres^{1,2}, M. Espanol², C. Persson¹, M.P Ginebra², M. Karlsson Ott¹

¹ [Materials in Medicine](#), Div. of Applied Materials Science, Dpt. Engineering Sciences, Uppsala University, Sweden. ² [Biomaterials, Biomechanics and Tissue Engineering](#), Dpt. Materials Science and Metallurgy, Technical University of Catalonia, Spain.

INTRODUCTION: Biomaterials can be designed to encourage wound healing by eliciting an appropriate immune response at the site of implantation [1]. The surface properties of calcium phosphate cements (CPCs), which have been the focus of many studies for bone regeneration, have been shown to play an active role in the cell response *in vitro* [2]. However, few studies have been done in regard to immune response. Thus the goal of this work was to study monocyte/macrophage proliferation and activation in response to topographically different CPCs. This is of particular interest since monocytes and macrophages are known to be crucial mediators of the host response to biomaterials, and their level of activation can be affected by material properties.

METHODS: α -tricalcium phosphate was milled using two different protocols to produce powder with different median particle size, 5.2 and 2.8 μm , coded as coarse (C) and fine (F), respectively [3]. 2 wt % of precipitated hydroxyapatite was added as a seed to the powder. Cements were prepared by mixing the powder with an aqueous liquid phase (2.5 wt% Na_2HPO_4) in a liquid to powder ratio of 0.65 ml/g. The cements were set in Ringer's solution (0.9 wt% NaCl) for 10 days, rinsed with milliQ water, and finally dried at 37°C overnight. Herein, the nomenclature used will be C-CPC and F-CPC. C-CPC resulted in platelet-like crystals while F-CPC produced needle-like crystals [3].

Cell proliferation on cements was evaluated by seeding $6 \cdot 10^4$ macrophages (Raw 264.7) on cement disks ($\varnothing=15\text{mm}$). Media were changed daily. After 1, 3 and 7 days the cells were lysed and lactate dehydrogenase (LDH) released was quantified. Moreover, the cells were treated with live/dead stain and observed by optical microscopy. Immune response was determined by exposing $2 \cdot 10^5$ monocytic cells (THP-1) to disks ($\varnothing=6\text{ mm}$) after which the release of reactive oxygen species (ROS) was studied using a luminol amplified chemiluminescence assay.

RESULTS: The number of cells on C-CPC after 1 and 3 days, as determined by LDH, was approximately twice as many as compared to F-

CPC. After 7 days, the differences were even larger; 10 times more cells were observed on C-CPC as compared to F-CPC. The cells attached on the cements were also visualized by live/dead stain (Fig. 1).

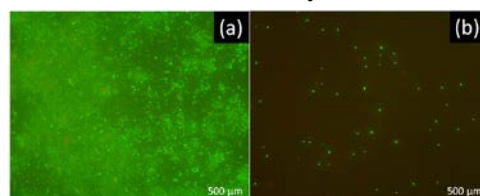


Fig. 1: Images of RAW 264.7 cells treated with live/dead stain on a) C-CPC and b) F-CPC after 7d.

Regarding the inflammatory response, F-CPC caused a lower production of ROS than C-CPC (Fig. 2).

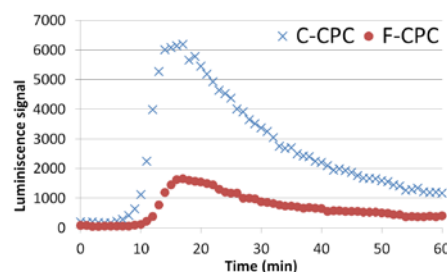


Fig. 2: Chemiluminescence measured over time for THP-1 cells exposed to C-CPC and F-CPC.

DISCUSSION & CONCLUSIONS: The lower number of cells present on F-CPC versus C-CPC is likely due to the fact that the needle-like crystals on the F-CPC surface do not favour cell attachment. Furthermore, the topography of the cements also caused a difference in activation of the THP-1 cells, where the plate-like crystals caused a higher production of ROS. Whether this is due to the fact that more cells attach to the C-CPC and thus give a higher total ROS production or is directly related to the morphology of the surface needs to be further evaluated.

REFERENCES: ¹ S. Franz, et al (2011) *Biomaterials* **32**:6692-6709. ² E. Engel, et al (2008) *Tissue Eng A* **14**:1341-51. ³ M. Espanol, et al. (2009) *Acta Biomater* **5**:2752-62.

ACKNOWLEDGMENTS: The authors would like to thank the Swedish Foundation for International Cooperation in Research and Higher Education (STINT), project IG2011-2047.

Bone-structural mimicry of TiO₂ scaffolds for regeneration of alveolar defects

B Müller¹, J Wengenroth², H Tiainen¹, H Haugen¹, SP Lyngstadaas¹

¹ *Department of Biomaterials, Institute of Clinical Dentistry, University of Oslo, Norway*

² *Institute of Medical and Polymer Engineering, Technische Universität München, Germany*

INTRODUCTION: Guided tissue regeneration (GTR) with use of resorbable and non-resorbable membranes is today the gold standard in the treatment of osseous defects in alveolar bone and periodontal pockets. Both resorbable and non-resorbable membranes show several shortcomings. Therefore it is the aim of this study to create a scaffold with a graded porosity to emulate the trabecular and cortical structure. Latter structure should include a surface, which favours bone cell attachment and prevents soft tissue from ingrowth into the scaffold interior.

METHODS: Polymer sponge method [1] was used to produce porous titanium dioxide (TiO₂) scaffolds, representing the trabecular bone structure. Subsequently different combinations of dry and wet surface coatings were applied through either gently dipping or forced pressing the surfaces into a mixture out of loose TiO₂ and Polyethylene (PE) powder. A further sintering step removed the as porogen acting PE to generate porosity within the scaffold surface itself.

Scanning electron microscopy (SEM) was used to examine the surface structure on the micrometer scale. μ CT-measurements were conducted to assess the architecture of the produced scaffolds. Under compressive loading the scaffold's mechanical properties were tested.

A first *in-vitro* study culturing normal human osteoblasts on the created surfaces was performed. Confocal microscopy and SEM was used to assess the influence of surface texture on cell morphology and attachment after 1, 3 and 7 days of culture.

RESULTS: A water-TiO₂-PE ratio of 10:10:1 in combination with a 2-step coating process, comprising of pressing the scaffold in TiO₂/PE powder followed by a wet coating with the aforementioned ratio, were most promising with regard to surface morphology. SEM and confocal microscopy results after 7 days indicate that osteoblasts favour a dense surface structure with small voids and canyons exceeding not more than 200 μ m in width.

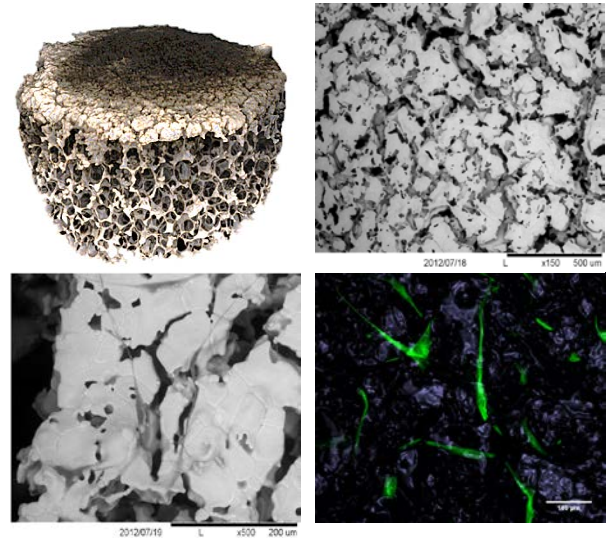


Fig. 1: 3D μ CT-image of the entire scaffold, SEM image of surface morphology, SEM and confocal microscope picture of osteoblasts attached to the cortical surface after 7 days of culture.

DISCUSSION & CONCLUSIONS: The comparison of different TiO₂/PE ratios highlighted the feasibility of creating a dense and the same time porous surface. 4 different coating procedures were compared regarding surface texture and *in-vitro* performance. Most promising osteoblast morphology was observed on a dense surface with single structural flaws smaller than 200 μ m since osteoblasts were able to bridge these distances. This surface was created with a double-layer coating procedure.

REFERENCES: ¹ Schwartzwalder, K., Somers, A.V., *Method of making porous ceramic articles*, General Motors Corporation, US Patent 3090094, 1963

ACKNOWLEDGEMENTS: Helen Pullisaar is gratefully acknowledged for her help in conducting the *in-vitro* study. Many thanks also to Esben Østrup for taking confocal microscope images.

Probing the biofunctionality of synthetically functionalized hyaluronan and chondroitin sulfate using biosensing techniques

E Nilebäck^{1,2}, N Altgårde¹, L de Battice¹, I Pashkuleva^{3,4}, J Becher⁵, S Möller⁵, M Schnabelrauch⁵, R L Reis^{3,4}, S Svedhem¹

¹ Chalmers University of Technology, Division of Biological Physics, Göteborg, Sweden. ² Biolin Scientific, Västra Frölunda, Sweden. ³ 3Bs Research Group-Biomaterials, Biodegradables and Biomimetics, University of Minho, Guimarães, Portugal. ⁴ ICVS/3B's—PT Government Associate Laboratory, Braga/Guimarães, Portugal, ⁵ Biomaterials Department, INNOVENT e.V., Jena, Germany

INTRODUCTION: Glycosamino glycans (GAGs) are native components of the extra-cellular matrix (ECM). Hyaluronan (HA) and chondroitin sulfate (CS) are both GAGs that can be functionalized in order to further apply them in e.g. tissue engineering applications. However, it is vital that the functionalization does not affect their biofunctionality in an undesired way. Here, HA and CS with varying degree of sulfation were biotinylated to enable their surface immobilization and subsequent biosensing of their interactions to ECM components. To probe their retained biofunctionality hyaluronidase degradation was used. Hyaluronidase is an enzyme known to degrade both HA and CS in the ECM.

METHODS: In order to use quartz crystal microbalance with dissipation monitoring (QCM-D) and surface plasmon resonance (SPR), biotinylated GAGs were immobilized to biotinylated self-assembled layers.¹ The obtained GAG surfaces were subjected to either hyaluronidase or aggrecan under liquid flow and detected by QCM-D or SPR. Hyaluronidase degradation was also studied in bulk conditions using high-performance liquid chromatography (HPLC).

RESULTS:

Table 1. Relative amounts of GAGs degraded by hyaluronidase in QCM-D (n=3)

	Biotin position	Sulfation Degree	Relative degradation
HA	End-on	0	0.80±0.04
HA	Side-on	0	0
CS	Side-on	0.9	0.65±0.05
Sulfated-CS	End-on	3.4	Enzyme adsorbed

DISCUSSION & CONCLUSIONS:

The results (Table 1) demonstrate that the functionalization greatly affected the biofunctionality of the surface-grafted GAGs. The biotin position (fig. 1) influences significantly the degree of degradation of HA, with side-on position leaving the GAG inert to degradation while end-on was degraded to 80 %.

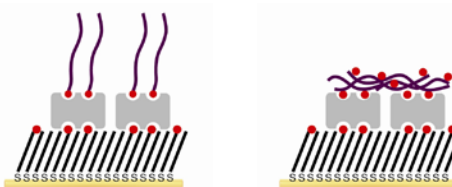


Fig. 1: End-on (left) and side-on (right) grafted biotinylated (red dots) GAGs

The importance of grafting orientation has also been addressed in a recent study on CS bound to supported lipid bilayers.²

Additional sulfation of CS induced adhesion of hyaluronidase, indicating that the function of the CS had substantially changed, highlighting the influence of sulfate group positions.

Further studies including interaction with the proteoglycan aggrecan and adhesion of chondrocytes will be conducted to further correlate the degradation response to biological function.

REFERENCES: ¹ E. Nilebäck, L. Feuz, H. Uddenberg, R. Valiokas, S. Svedhem, (2011) *Biosensors and Bioelectronics* **28**, 407-413, ² N. Altgårde, J. Becher, S. Möller, F. E. Weber, M. Schnabelrauch, S. Svedhem, (2013) *Journal of Colloid and Interface Science* **390**, 258-266,

ACKNOWLEDGEMENTS: The research leading to these results has received funding from the European Union Seventh Framework Programme (FP7/2007-2013) under grant agreement no NMP4-SL2009-229292 ("Find & Bind").

Porosity prediction of calcium phosphate cements

C Öhman¹, E Carlsson¹, MP Ginebra², C Persson¹, H Engqvist¹

¹ Div. of Applied Materials Science, Dept. of Engineering Sciences, Ångström Laboratory, Uppsala University, Sweden. ² Biomaterials, Biomechanics and Tissue Engineering Group, Dep. of Materials Science and Metallurgy, Technical University of Catalonia (UPC), ETSEIB, Spain

INTRODUCTION: For all ceramic cements it is important to have control over and be able to predict the porosity in the hardened body. The amount of pores influences several important parameters, such as mechanical properties, resorbability and bioactivity.

Powers and Brownyards¹ developed a model that predicts porosity on the basis of cement composition and water to cement ratio. The aim of the present study was to use Powers and Brownyards model as a base for developing a model to predict porosity of calcium phosphate cements. Furthermore, the model was verified with experimental tests.

METHODS: The porosity in the hardened cement will be governed by the initial water to cement ratio in the cement paste. The amount of cement that will dissolve depends on: 1) the water to cement ratio (w/c) in the mixture; and 2) the volume water needed to dissolve one unit volume of cement.

The water volume needed (k) and the volume of hydrates formed (s) can be calculated based on the chemical reaction of the cement and the molar weight and density of the different components.

The volume of the sample not filled with cement or hydrates will be empty, i.e. pores. The volume fraction of pores will be:

$$\Phi_p = \frac{1 + w/c - V_c - V_h}{1 + w/c} = \begin{cases} \frac{1 + k - s}{1 + w/c} \cdot \frac{w/c}{k}, & w/c < k \\ 1 - \frac{s}{1 + w/c}, & w/c > k \end{cases} \quad (1)$$

60 m% β -TCP and 40 m% MCPM were hand-mixed with deionized water, at liquid-to-powder (L/P) ratios of 0.4, 0.5, 0.6 or 0.7 ml/g. 20 samples of each L/P were prepared. Samples were set for 24 hours at 37 °C and 100% RH. Thereafter, samples were dried at 37 °C for 7 days. Helium pycnometry was used to determine the skeletal density and together with specimen mass and dimensions, the porosity could be determined.

RESULTS: For the present quantities of β -TCP and MCPM it was found that $k=0.83$ and $s=1.56$.

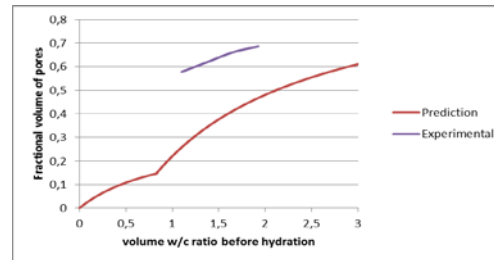


Fig. 1: Predicted and experimental porosity for different w/c ratios of brushite.

Weight loss of the specimens was observed during drying, which might indicate a phase transformation from brushite to monetite. Changing the outcome of the chemical reaction to monetite gave $k=0.07$ and $s=0.98$.

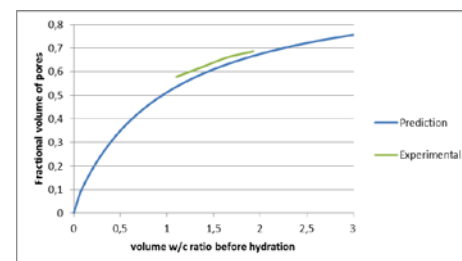


Fig. 2: Prediction and experimental porosity for different w/c ratios of monetite.

DISCUSSION & CONCLUSIONS: Further studies are needed to verify and quantify the phase transformation. The difference between experimental and predicted values could be due to manual mixing before moulding, which will introduce pores to the final product. Nevertheless, this study shows a model that could be used to predict porosity of calcium phosphate cements.

REFERENCES: ¹ T.C.Powers, T.L.Brownyards (1948) *Studies of the physical properties of hardened cement paste*, Publication of Research Laboratories of the Portland Cement Association, Chicago USA.

ACKNOWLEDGEMENTS: This work was partially supported by Stiftelsen Lars Hiertas minne and the Swedish Foundation for International Cooperation in Research and Higher Education (STINT).

Identification of functional structures in tissue engineered cartilage: from nm- to macro scale.

MØ Olderøy¹, M Sandvold², FP Reinholt³, M Lilledahl², P Sikorski², JE Brinchmann¹

¹ [Norwegian Center for Stem Cell Research](#), Oslo University Hospital, Oslo, Norway.

² [Department of Physics](#), Norwegian University of Science and Technology, Trondheim, Norway.

³ [Department of Pathology](#), Oslo University Hospital, Oslo, Norway

INTRODUCTION: Tissue engineering of cartilage requires the combination of a cell type with suitable genetic profile and a biomaterial which allows for development of a functional construct. In the literature, the focus has primarily been on cell differentiation and secretion of relevant extracellular matrix (ECM) proteins, combined with mechanical analysis of the final construct. Although the source of functional properties must originate from the interaction between ECM molecules and their structures over several length scales, the assembly of type II collagen and aggrecan into higher order structures has not received much attention. We have applied a range of advanced imaging technologies to address functional structures of relevant ECM molecules in tissue engineered cartilage, where mesenchymal stem cells (MSC) are undergoing chondrogenic differentiation in alginate hydrogels.

METHODS: MSC undergoing differentiation for up to six weeks in alginate hydrogels were characterized by a range of imaging technologies, including transmission electron microscopy (TEM), high resolution 3D tomography based on focused ion beam/scanning electron microscopy (FIB/SEM), non-linear confocal microscopy (SHG) and immunohistochemical (IHC) staining.

RESULTS: TEM provides high resolution imaging of individual ECM components and cells (2D, resolution ~1 nm), while FIB/SEM allows for high resolution reconstruction of tissue volumes, allowing us to follow individual collagen fibrils through the material (3D, resolution ~10 nm), to investigate cellular structures and visualize cell-matrix interface in unprecedented details. SHG specifically images organized fibrillar collagen, which was compared to IHC, where the mere presence of ECM molecules is detected and imaged. In combination, these techniques provide novel insights into the architecture of the forming tissue as well as input for tissue engineering strategies. Particularly collagen and aggrecan structures are important in articular cartilage. Here, focus is mainly on collagen structures and

their location through the tissue engineered material. IHC staining (Fig. 1c) of type II collagen shows a relatively homogeneous distribution through the alginate hydrogels already after two weeks in culture. This contradicts the finding from SHG imaging (Fig. 1d), which indicates fibrillar collagen only in the pericellular region. Examination by TEM (Fig. 1a) and FIB/SEM microscopy (Fig. 1b) further indicate that collagen close to cells is fibrillar, while collagen located far from cells is not fibrillar. Collected FIB/SEM data allows for 3D reconstruction of selected areas of the sample, with visualization of complete collagen network in areas close to, and further away from cells.

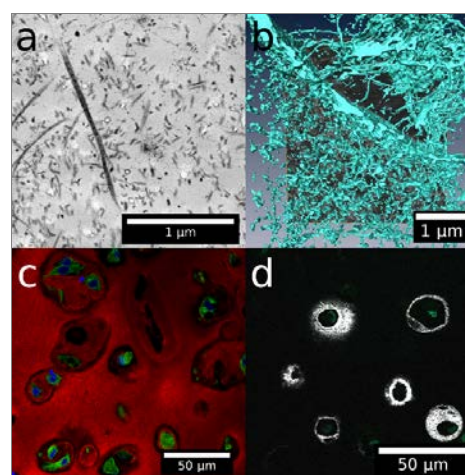


Fig. 1: (a) Individual collagen fibrils imaged by TEM, (b) 3D reconstruction based on FIB/SEM, (c) IHC localization of type II collagen (red), (d) SHG imaging of fibrillar collagen. Collagen is identified throughout material, however, fibrillar collagen is detected only close to cells.

DISCUSSION & CONCLUSIONS: Data indicates the importance of advanced imaging technologies as a tool to characterize the architecture of tissue engineered cartilage.

ACKNOWLEDGEMENTS: We acknowledge LT Dorg and SH Brorson for assistance with sample preparation for optical and electron microscopy, and NTNU Nanolab for access to FIB/SEM instrument.

Custom-made bone grafts for reconstructive maxillo-facial surgery: a case study

G. Pertici¹, F. Grecchi², G. Perale¹

¹ *Industrie Biomediche Insubri SA, Mezzovico, Switzerland.* ² *Istituto Ortopedico R. Galeazzi, Dept. of Maxillo-facial surgery, Milan, Italy.*

INTRODUCTION: Scaffolds for bone regeneration should ensure both mechanical stability and strength. Moreover, their intimate structure should have an adequate interconnected porous network for cell migration and proliferation, while also providing specific signals for bone regeneration. SmartBone[®] composite solution, based on a novel concept of biomaterial assembly, bearing cues from both mineral components and polymeric ones [1-3], was chosen to develop new patient-specific three-dimensional bone grafts. Indeed, thanks to mechanical performances and to full control over production, custom-made grafts can be produced according to the specific need of each single patient, via digital surgical planning, starting from CT scans.

METHODS: SmartBone[®] technology, a bovine derived mineral matrix reinforced with resorbable biopolymers and bioactive agents [1-3], was applied together with a CAD-CAM manufacturing system to obtain custom-made 3D bone grafts.

The case of a 38-years old Caucasian male with an important traumatic defect of his left zygomatic portion was here investigated: CT scans were acquired; surgical planning together with graft design was performed both on real model (made by 3DiEmme srl, Italy) and digitally (3Diagnosys software, by 3DiEmme srl, Italy); once surgical procedure and grafts had been confirmed, 5axes CAD-CAM manufacturing process (Industrie Biomediche Insubri SA, Switzerland) was used to machine-mill bovine derived mineral matrix into final shapes, which then underwent proprietary physical-chemical reinforcement process prior to packaging and sterilization [1].

After general anaesthesia, surgery began with site preparation along the old scar, including removal of formerly placed cartilage grafts and metal parts. Once receiving site had been properly prepared, custom-made grafts were placed and fixed with standard fixation tools (KLS Martin & Co. GmbH, Germany). Grafted bone substitutes were covered with long lasting resorbable collagen membranes (Tutomesch, by Tutogen Medical GmbH, Germany) and finally muscles and soft tissue layers were sutured back in place. Control CT scans were acquired 2 days and 6 months post surgery.

RESULTS: Surgical planning resulted in the need of three bone grafts: two for the external zygoma and one for orbital pavement, respectively (see Figure 1 left). Surgery was performed as planned and grafts fixation required just few minutes: only 5 screws and 1 plaque easily ensured proper grafts stability (see Figure 1 right).

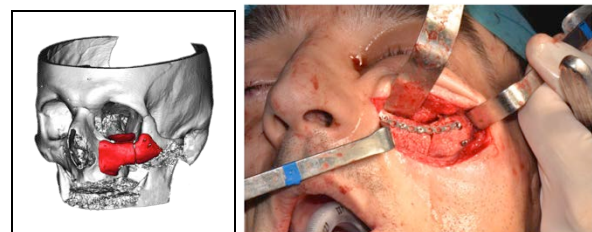


Fig. 1: left – digital planning of the needed grafts; right – surgical fixation of the grafts onto patient.

Facial symmetry was restored, together with a proper orbital alignment. No visual nor neurological outcomes were reported. Post surgical CT scans confirmed correct positioning of grafts (after 2 days) and confirmed graft integration and stability (after 6 months), showing no signs of bone graft volumetric reduction.

DISCUSSION & CONCLUSIONS: a proper surgical planning and a precise design of needed grafts allowed obtaining a very satisfactory reconstruction. SmartBone[®] technology proved being adequate: bone grafts showed extremely high mechanical performances, easily withstanding fixation manoeuvres, while material stability and integration were fully confirmed too.

Moreover, a correct and precise planning, the perfect geometrical matching of grafts with receiving site, ensured by the precise production, and a high performance bone graft, resulted in a relevant reduction of surgical time and, therefore, of surgery-related risks for patient.

REFERENCES: ¹ G. Pertici (2008) *Bone implant matrix and method of preparation of the same*, pat. appl. CH 01997/08. ² S. Bardelli *et al.* (2009) *Clinically-optimized cell culture conditions in combination with a new 3d-scaffold for human msc bone tissue engineering*, Reg. Med, 4(6)-s2:70-1. ³ G. Perale *et al.* (2010) *Bioresorbable bioactive matrix for bone regeneration*, Tissue Engineering Part A, 16(8): A-10.

Coating of titanium surfaces with Emdogain® by hydridation increased bone mineralization in vivo

C. Petzold¹, Marina Rubert², S. P. Lyngstadaas¹, Marta Monjo²

¹ University of Oslo, Oslo, Norway; ² University of Balearic Islands, Palma de Mallorca, Spain,

INTRODUCTION: Emdogain® (EMD) is a commercial product consisting of hydrophobic enamel matrix proteins extracted from porcine developing embryonic enamel¹. A positive effect on mineralization of bone tissue^{2,3} and reduced activity of osteoclastic cells⁴ were found in vitro. Stable layers of TiH₂ can be obtained on the surfaces of Ti by cathodic polarization⁵. Hydride ions may improve bone integration with the implant⁶. In order to combine the initial positive effect on bone mineralization of EMD with a good long-term integration of the implant in bone, Ti samples were coated with TiH₂ and 2 different concentrations of EMD. The surfaces were tested in vivo for bone-implant attachment strength, bone formation markers, and mineralization after 8 weeks of implantation in rabbits.

METHODS: Mirror polished and grit-blasted (GB) commercially pure (cp) Ti was coated with TiH₂⁵ for 5 h (H). EMD was added to the electrolyte after 5 h for 1 h (EMD 0.02: 0.02 mg ml⁻¹; EMD 0.1: 0.1 mg ml⁻¹). The surfaces were characterized with SEM and the amount of EMD attached to the surfaces was quantified in a release study (BCATM Protein Assay Kit). The Ti samples were implanted in the tibiae of rabbits in a bone chamber model⁷. After 8 weeks, the bone-to-implant attachment strength, LDH and total protein in the wound fluid, and the expression of mRNA markers in the peri-implant bone tissue were analyzed. Further, the bone volume (%BV) in the defect was quantified by micro-CT.

RESULTS: Detectable amounts of EMD were released from the coated Ti surfaces and a higher amount of EMD was measured if a lower concentration of EMD had been used in the electrolyte (Table 1).

Table 1. Release of EMD from coated Ti surfaces.

	EMD 0.02	EMD 0.1
Mean ± SD	18.7 ± 2.6	9.3 ± 5.3

The pull-out forces were in the range of 27.8 ± 11.3 N without significant differences between the groups. The inflammatory marker IL-6 was increased on EMD 0.1 compared to H and EMD 0.02. Coll-1, a marker for early bone formation

was significantly decreased for EMD 0.02 compared to H. For Runx2, a significantly lower level was found for EMD 0.02 compared to EMD 0.1. The expression of OC, a marker for bone mineralization, was significantly reduced for EMD 0.02 compared to EMD 0.1. No significant differences were found for the osteoclast marker TRAP. A significantly higher %BV was found for EMD 0.02 compared to EMD 0.1 (Fig. 1).

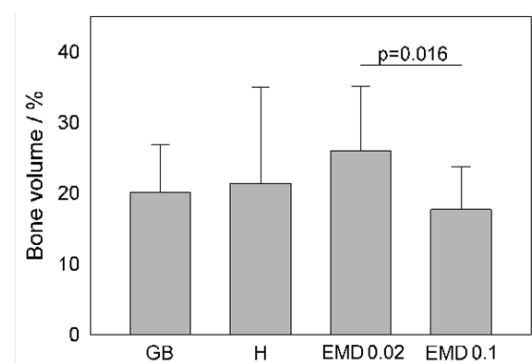


Fig. 1: An increased bone volume was found in the defects that were covered with Ti coated with EMD of lower concentrations as measured with micro-CT.

DISCUSSION & CONCLUSIONS: Coating of Ti with TiH₂ and an additional layer of EMD was possible by cathodic polarization. The EMD was reversibly attached and thus readily available for cells in vivo. Lower expression of bone formation markers in the peri-implant bone tissue together with a higher percentage of bone in the defect indicate a more readily bone mineralization for EMD 0.02. The use of higher concentrations of EMD resulted in increased inflammatory levels and lower percentage of mineralized bone tissue. The effects behind the counterintuitive release should be further elucidated.

REFERENCES: ¹ M. Zeichner-David (2001) *Matrix Biology* 20:307. ² Z. Schwartz et al (2000) *J Periodontol* 71:1287. ³ P. Weishaupt et al (2008) *Oral Surg Oral Med Oral Pathol Oral Radiol Endod* 106:304. ⁴ M. Nishiguchi et al (2007) *Archives of Oral Biology* 52:237. ⁵ K. Videm et al. (2008) *Applied Surface Science* 255:3011. ⁶ Z. Cheng et al (2010) *Oral Surg Oral Med Oral Pathol Oral Radiol Endod* 110:e5. ⁷ M. Monjo et al (2010) *Acta Biomaterialia* 6:1405.

Coating titanium dioxide scaffold with simvastatin in alginate promote osteoblast differentiation in vitro

H Pullisaar¹, E Østrup^{1,2}, H Tiainen¹, M Landin³, SP Lyngstadaas¹, JE Reseland¹, HJ Haugen¹

¹ Department of Biomaterials, Institute of Clinical Dentistry, University of Oslo, Norway.

² Norwegian Center for Stem Cell Research and Institute of Immunology, Oslo University Hospital Rikshospitalet, University of Oslo, Norway. ³ Clinical Oral Research Laboratory, Institute of Clinical Dentistry, University of Oslo, Norway.

INTRODUCTION: Statins, 3-hydroxy-3-methylglutaryl-coenzyme A reductase inhibitors, are widely used for lowering serum cholesterol level in hypercholesterolemia. Furthermore, additional pleiotropic effects of statins such as antiresorptive and anabolic effects on bone have been described.

The aims of this study was to develop a method for coating titanium dioxide (TiO₂) scaffolds with alginate hydrogel containing simvastatin (SIM), and to examine the effect of controlled release of SIM on bone formation.

METHODS: TiO₂ scaffolds, produced by polymer sponge replication as previously described [1], were submerged into 2 % alginate solution containing either 10 nM or 10 μM SIM followed by centrifugation to remove the excess alginate solution. Subsequently, scaffolds were immersed into 50 mM CaCl₂ to allow gelation. Scaffolds were finally rinsed with dH₂O and let to dry overnight at room temperature. The microstructure of resulting composite scaffolds was visualized by scanning electron microscopy (SEM) and Periodic acid-Schiff (PAS) staining. The SIM release was measured by UV-Vis spectroscopy. Primary human osteoblast cells were seeded onto scaffolds and cultured for 21 days. Cell viability was evaluated by determination of lactate dehydrogenase (LDH) activity in culture medium. Expression of osteoblast markers was investigated using real-time RT-PCR, and secretion by Luminex.

RESULTS: The described immersion-centrifugation technique resulted in an evenly distributed alginate layer coating the entire surface of the TiO₂ scaffold struts (Fig.1 A-C). Sustained SIM release was observed for up to 19 days. No cytotoxic effects were observed by scaffolds coated with alginate hydrogel containing either 10 nM or 10 μM SIM compared to uncoated scaffolds. Osteocalcin, one of the most specific late expressed osteoblast markers, was significantly enhanced by scaffolds coated with

alginate hydrogel containing 10 μM SIM compared to 10 nM SIM and uncoated scaffolds at 21 day.

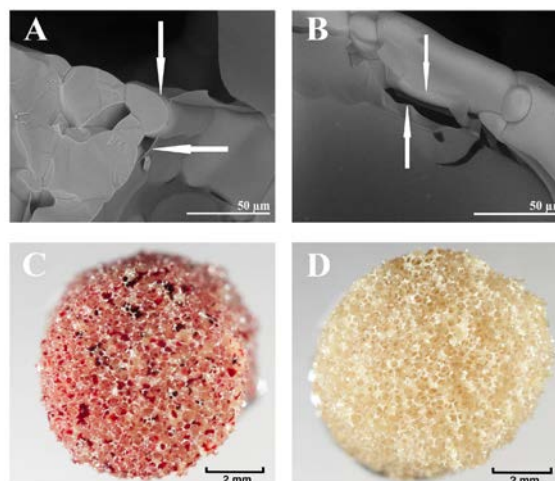


Fig. 1: SEM visualization of alginate layer (arrows) coating the TiO₂ scaffolds (A, B) and PAS staining of alginate coated scaffold (C) and uncoated scaffold (D).

CONCLUSIONS: Our study shows that alginate-coated TiO₂ scaffolds can act as a matrix for delivery of SIM, inducing osteoblast cell differentiation. The combination of the physical properties of TiO₂ scaffolds with the osteogenic effect of SIM may represent a new strategy for bone tissue regeneration in load-bearing applications.

REFERENCES: ¹ H. Tiainen, SP. Lyngstadaas, JE. Ellingsen, HJ. Haugen (2010) *J Mater Sci Mater Med.* **21** (10):2783-92.

ACKNOWLEDGEMENTS: This study was supported by Eureka-Eurostars Project Application E!5069 NewBone.

Strontium ranelate treatment increases the formation of bone-like mineralized matrix by osteoblast cells cultured onto pure titanium substrates

William Querido^{1,2}, Leida G Abraçado¹, Karine Anselme², Marcos Farina¹

¹ Instituto de Ciências Biomédicas, Universidade Federal do Rio de Janeiro, Rio de Janeiro, Brasil.

² Institut de Sciences des Matériaux de Mulhouse (IS2M), CNRS LRC7228, Université de Haute-Alsace, Mulhouse, France.

INTRODUCTION: Strontium ranelate is a drug used for treating women with postmenopausal osteoporosis¹. Additionally, in the last few years, new promising applications of the drug are being suggested. In particular, strontium ranelate was shown to improve the osseointegration of implants^{2,3,4}. The better understanding of this process could play relevant roles on future applications of the drug on bone tissue engineering approaches. The goal of this study was to evaluate the effects of strontium ranelate treatment on the formation of bone-like mineralized matrix by osteoblast cells cultured onto titanium substrates.

METHODS: Murine F-OST osteoblast cells were cultured for 28 days onto polished pure titanium substrates under mineralizing conditions (10 mM β -glycerophosphate and 50 μ g/mL ascorbic acid) and treatment with strontium ranelate (PROTOS®, Servier Laboratories) at 0.5 mM Sr^{2+} . The titanium substrates were characterized by scanning electron microscopy (SEM) with energy-dispersive X-ray spectroscopy (EDS) and atomic force microscopy (AFM) using the Nova software. The mineralized area found on the surface of the substrates was evaluated with the ImageJ software. The nature and composition of the matrix was analyzed by Alizarin Red S staining, Fourier transform infrared spectroscopy (FTIR) operating on the attenuated total reflection (ATR) mode, and EDS.

RESULTS: The substrates were characterized as pure titanium presenting average roughness (Sa) of 123 ± 31 nm. Both in control and treated cultures, the osteoblast cells produced a mineralized matrix onto the titanium substrates, seen as white deposits that were stained in red by Alizarin Red S staining for calcium. It was clear by crude observation that strontium ranelate treatment led to a more extensive mineralized matrix formation onto the substrates (Fig. 1). Accordingly, the substrate surface area occupied by mineralized matrix was significantly increased in treated cell cultures ($P < 0.01$). The nature of the mineralized matrix revealed by ATR-FTIR analysis was similar in control and treated cultures. The spectra comprised typical bands of PO_4^{3-} and CO_3^{2-} described in bone

apatite and of Amide I and II from peptide bonds found in collagen. In both cases, the mineralized matrix produced in culture was similar to that described in native bone tissue. In both control and treated cultures, the mineralized matrix presented Ca and P as main chemical components, as seen by EDS analysis. Although not detected in control, the presence of Sr was clearly seen in treated cultures, indicating that Sr was incorporated into the mineralized matrix produced under strontium ranelate treatment.

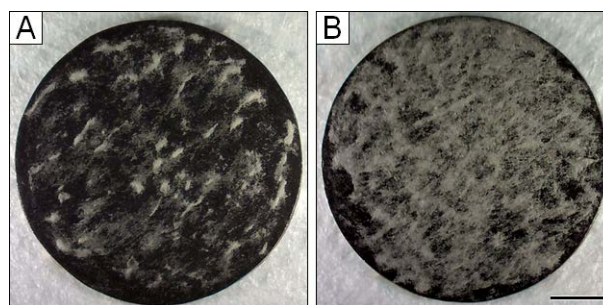


Fig. 1: Mineralization onto titanium substrates in (A) control and (B) treated osteoblast cell cultures. Scale bar: 2mm.

DISCUSSION & CONCLUSIONS: Strontium ranelate treatment increased the formation of bone-like mineralized matrix by osteoblast cells cultured onto pure titanium substrates. Moreover, Sr was incorporated into the matrix produced under treatment. In order to reveal possible applications of strontium ranelate on bone tissue engineering approaches, a detailed evaluation of its effects on the interaction of cells with biomaterials presents an interesting subject for further studies.

REFERENCES: ¹ P.J. Marie (2006) *Curr Opin Rheumatol* **18** Suppl 1:S11-5. ² L Maimoun, TC Brennan, I Badoud, et al (2010) *Bone* **46**(5):1436-41. ³ Y Li, G Feng, Y Gao, et al (2010) *J Orthop Res* **28**(5):578-82. ⁴ Y Li, X Li, G Song, et al (2012) *Clin Oral Implants Res* **23**(9):1038-44.

ACKNOWLEDGEMENTS: This study was supported by FAPERJ, CNPq, and CAPES (Brazil).

Increased hydride in titanium surfaces after cathodic polarization in organic acids promote gingival fibroblast growth independent of surface complexity and wettability

R Xing, S Taxt-Lamolle, L Salou, JE Reseland, HJ Haugen, SP Lyngstadaas

Department of Biomaterials, Institute for Clinical Dentistry, University of Oslo, Oslo, Norway.

INTRODUCTION: Peri-implant mucosal attachment surrounding the dental abutment is an important factor for long term success of implants. Several efforts have previously been made to optimize the abutment surfaces, but no consensus has been reached regarding the optimal architecture and composition for soft tissue growth and attachment. A successful approach using cathodic polarization in acid has been used to optimize titanium implant surfaces for improved osseointegration. However, the effect of surface changes from cathodic polarization on the performance of titanium abutment surfaces has so far not been studied.

METHODS: Here we employed cathodic polarization to modify titanium (Ti) surfaces, following a previous study [1]. Three different organic electrolytes were used: oxalic acid, tartaric acid and acetic acid. Reaction durations varied from 0.5 h to 5 h and current density from 1 mA/cm² to 15 mA/cm². Surface topography was analyzed by blue light profilometer, field emission scanning electron microscopy (FE-SEM) and atomic force microscopy (AFM). Secondary ion mass spectrometry (SIMS) was used to quantify elemental compositions on the surfaces. Hydrophilicity was determined by contact angle measurement. Samples were evaluated *in vitro* performances using human gingival fibroblasts (HGF) by studying cell viability, morphology and proliferation rates at different time points.

RESULTS: Three main factors affecting the surface topography and chemistry were the electrolyte composition, the current density and the polarization time. At 15 mA/cm² for 5 hours, oxalic acid in the electrolyte created rougher surfaces than tartaric acid and acetic acid (Fig. 1). Under identical conditions, acetic acid produced the highest hydride amount in the surfaces. Due to decreasing current efficiency, hydride first increase and then decrease with higher current density. In oxalic acid, the 5 mA/cm² current density produced more hydride than 15 mA/cm² after 5 hours. The complexity (S_a , S_{dr}) of the

surface topography and hydride production both increased with increasing polarization time.

The modified Ti surfaces showed low cytotoxicity and increased HGF proliferation rates after three days *in vitro* compared to polished surfaces. Proliferation rate of human gingival fibroblasts at day 3 was positively correlated with the surface hydride content. However, surface roughness and hydrophilicity did not significantly influence the growth of HGF cells.

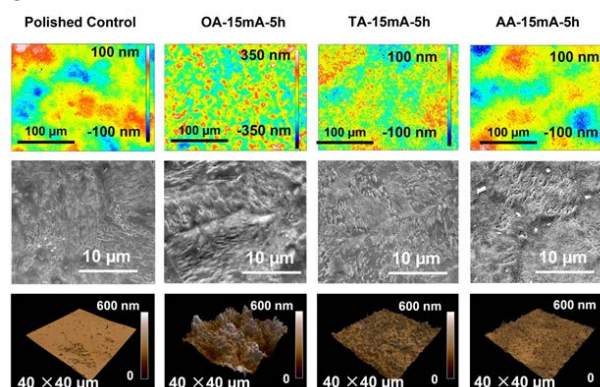


Fig. 1: Surface topography of samples produced in different acids at 15 mA/cm² for 5 h.

DISCUSSION & CONCLUSIONS: Hydride amount and surface topography were influenced by the nature of organic electrolytes, current density and polarization time. Acetic acid implemented highest hydride amount compared to oxalic acid and tartaric acid, while oxalic acid resulted in most complex surface topography. Hydride content increased along with polarization time, while it started to decrease with current density after reaching a peak. HGF growth was enhanced on Ti surfaces modified by cathodic polarization. The improved performance was suggested to be due to increased hydride content, rather than changes of surface complexity or hydrophilicity.

REFERENCES: [1] Ellingsen JE, Videm K, Opsahl L, Ronold HJ. Implants with modified surfaces for increased biocompatibility, and method for production thereof. US Patent No. 6,627,3212003.

UV photoactivation of 7-dehydrocholesterol on titanium implants enhances osteoblast differentiation and decreases *Rankl* gene expression

M Satué¹, C Petzold², A Córdoba¹, JM Ramis¹ and M Monjo¹

¹[Research Institute on Health Sciences \(IUNICS\)](#) University of Balearic Islands, Palma de Mallorca, Spain. ²[Department of Biomaterials](#). Institute for Clinical Dentistry, University of Oslo, NO.

INTRODUCTION: Vitamin D plays a central role in bone regeneration and its insufficiency negatively affects bone regeneration, including implant osseointegration [1]. Ti is the material most commonly used for bone implants because of its physical and biological properties [2]. Current dental implant research aims to produce innovative surfaces promoting a favorable biological response and a rapid osseointegration. UV-activated provitamin D3 coating on Ti surfaces is here suggested to have a stimulatory effect on bone cells and accelerate bone regeneration as result of active vitamin D synthesis.

METHODS: Titanium disks were coated with 7-dehydrocholesterol dilution and then allowed to air-dry until UV-irradiation. A 302 nm UV lamp was used for the photoactivation process during different UV time exposures. FTIR analysis and HPLC were used to characterize and quantify the conversion of 7-DHC to previtamin D3. Cytotoxicity, alkaline phosphatase (ALP) activity, calcium (Ca) content, 25-hydroxyvitamin D3 (25-D3) production, gene expression of bone markers and enzymes involved in vitamin D3 synthesis were analyzed using MC3T3-E1 cells as an *in vitro* model.

RESULTS: FTIR results showed changes in the ring structure resulted from the 7-DHC conversion into previtamin D3. HPLC analysis determined a $16.5 \pm 0.9\%$ conversion of 7-DHC to previtamin D3 after 15 min of UV exposure, and a $34.2 \pm 4.8\%$ of the previtamin D3 produced was converted to 25-D3 by the osteoblastic cells. No cytotoxic effect was found for Ti implants treated with 7-DHC and UV-irradiated. Moreover, Ti implants treated with 7-DHC and UV-irradiated for 15 min showed increased 25-D3 production, together with increased ALP activity and calcium content (Figure 1). Interestingly, *Rankl* gene expression was significantly reduced in osteoblasts cultured on 7-DHC coated Ti surfaces when UV-irradiated for 15 and 30 minutes to $33.56 \pm 15.28\%$ and $28.21 \pm 4.40\%$ respectively when compared to control.

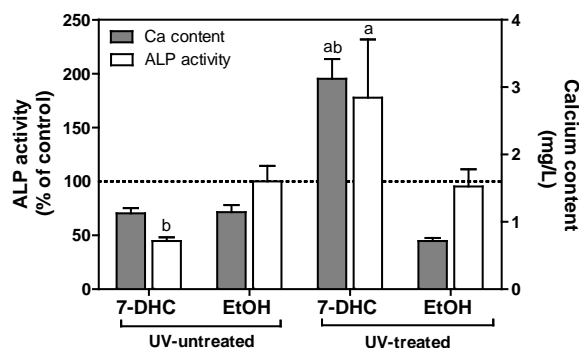


Fig. 1: Effect of 7-DHC and UV exposure of Ti implants on ALP activity and mineralization.

ALP activity measured at 21 days and Ca content measured at 28 days of MC3T3-E1 culture. Mann-Whitney test ($p < 0.05$): ^aUV-treated vs. UV-untreated for 7-DHC and ethanol, respectively; ^b7-DHC treatment vs. the corresponding ethanol control.

DISCUSSION & CONCLUSIONS: Our results show for the first time the use of UV-activated 7-DHC to locally produce cholecalciferol at the surface of the titanium implant which increases *in vitro* osteoblast differentiation as result of the endogenous synthesis of active vitamin D [3].

REFERENCES: ¹G. Dvorak, A. Fögl, G. Watzek, S. Tangl, P. Pokorny, R. Gruber (2011) *Clin Oral Implants* **23**:1308-1313. ² J. Kelly, A. Lin, CJ. Wang, S. Park, I. Nishimura (2009) *J Prosthodont* **18**:473-478. ³ M. Satué, C. Petzold, A. Córdoba, J.M. Ramis, M. Monjo (2012) *Acta Biomater* Doi: 10.1016/j.actbio.2012.11.021.

ACKNOWLEDGEMENTS: This work was supported by the MICINN (Torres Quevedo contract to JMR, and Ramón y Cajal contract to MM) and Eureka-Eurostars Project Application E!5069 NewBone, Interempresas International Program (CIIP20101024) from the CDTI, Invest in Spain (C2_10_32) and European Regional Development Fund.

Intracellular signaling in osteoblasts on regularly structured titanium surfaces

S Staehlke¹, F Kunz², R Loeffler³, C Matschegewski¹, M Fleischer³, DP Kern³, JB Nebe¹

¹University Medical Center Rostock, Department of Cell Biology, Rostock, GER. ²University of Rostock, Faculty of Computer Science and Electrical Engineering, Institute of General Electrical Engineering, Rostock, GER. ³University of Tuebingen, Institute for Applied Physics, Tuebingen, GER

INTRODUCTION: Implant characteristics like surface chemistry and topography affect the behavior of cells [1]. The adhesion of cells at the surface of an implant triggers a cascade of intracellular events modulating cell functions like growth and proliferation [2]. Ca^{2+} as a ubiquitous second messenger plays a key role in intracellular signaling, controlling many cellular processes like gene expression, mitosis and cell death. Regulation of cytoplasmic Ca^{2+} concentration involves calcium channels [3]. We know that the formation of intracellular adhesion components such as the actin cytoskeleton is altered in response to the surface topography [4]. But how these structural changes influence intracellular signaling is largely unknown. This study is intended to elucidate such effects using regular pillar structures to characterize the modulation of cell responses like activation of signaling molecules as well as the regulation of calcium channels in osteoblasts.

METHODS: Arrays of cubic pillars of SU-8 (Microchem) with dimensions of $5 \times 5 \times 5 \mu\text{m}^3$ (LxWxH) were obtained on silicon wafers by a photolithographic process. A planar substrate was used as control. Both investigated discs were sputter-coated with titanium (100 nm). Human osteoblastic cells (MG-63, ATCC) were cultured in DMEM with 10 % FCS (PAA) over periods ranging from 5min to 24h in order to investigate the time dependent phosphorylation state of signaling proteins of the MAPK-cascades. The phosphorylation of the signaling protein was examined by an xMAP™ Luminex assay (Bio-Rad). Immunofluorescence analyses for the expression of calcium channels after 24h were performed by confocal laser scanning microscopy and FACSCalibur flow cytometry.

RESULTS: Concerning the activation of signaling proteins the data implicates that p-MEK1 and p-ERK1/2 were modulated in a time dependent manner. The p-MEK1 already increased in the initial phase of cell adhesion (10min) on the pillar structure compared to the planar reference.

Furthermore osteoblastic cells expressed the most common subtypes of L- and T-type voltage-sensitive calcium channels ($\text{Ca}_v1.2$ and $\text{Ca}_v3.1$). The spatial distribution of the calcium channels is not altered by the underlying surface microstructure (Fig. 1).

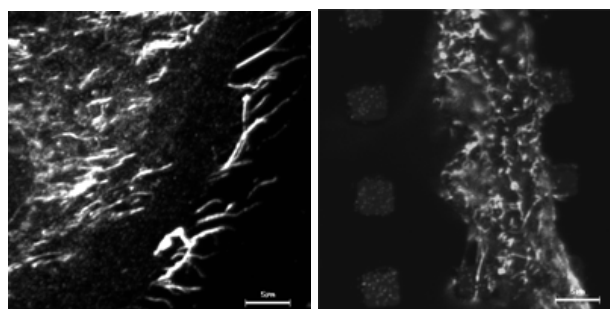


Fig. 1: Confocal microscopy images of the distribution of calcium channel $\text{Ca}_v3.1$ (left) on planar reference and (right) on pillar structures in osteoblasts (zoom scale bar = $5 \mu\text{m}$).

DISCUSSION & CONCLUSIONS: These data indicates that the signaling pathways are likely partially topographically sensitive. The localisation of calcium channels on the microstructures revealed no obvious differences prior to functional analysis. The biocomplexity of regulatory cellular pathways in response to the biomaterial's influence is a challenge and of clinical relevance for the development of optimal implant designs in regenerative medicine.

REFERENCES: ¹ F Luethen et al. (2005) *Biomaterials* **26**(15): 2423-40. ² DW Hamilton & DM Brunette (2007) *Biomaterials* **10**:1806-19. ³ LM Walker et al. (2000) *J Cell Biochem* **79**(4): 648-61. ⁴ C Matschegewski et al. (2010) *Biomaterials* **31**(22): 5729-40.

ACKNOWLEDGEMENTS: SS, FK, RL and CM are grateful for the financial support of the Deutsche Forschungsgemeinschaft (DFG) (NE 560/7-2, KE 611/7-2) as well as of the DFG graduate school welisa (1505/1).

Amorphous degradable poly(L-lactide-co-caprolactone) scaffold fabricated by Three Dimensional Fiber Deposition method

Yang Sun¹, Kamal Mustafa², Ann -Christine Albertsson¹, Dirk W Grijpma³, Lorenzo Moroni⁴, Wim J Hendrikson⁴, Anna Finne-Wistrand*¹

¹Dept. of Fibre and Polymer Technology, KTH Royal Institute of Technology, Stockholm, Sweden

²Dept. of Clinical Dentistry-Center for Clinical Dental Research, University of Bergen, Norway

³MIRA Institute for Biomedical Technology and Technical Medicine, Dept. of Polymer Chemistry and Biomaterials, University of Twente, The Netherlands

⁴Department of Tissue Regeneration, University of Twente, The Netherland

INTRODUCTION: Polymers such like amorphous copolymer of poly(L-lactide-co-caprolactone) is a very elastic material and showed many positive results in bone tissue engineering applications¹⁻². Comparing with its homo-polymer, the copolymer could bear strenuous bending and compression without breaking³. For tissue engineering, we are making efforts to produce interconnected 3D scaffolds for cell carrier. Moreover, the scaffolds should be fabricated in a reproducible way with optimized mechanical properties and cell distribution. For this purpose, a melt-based 3D Fiber Deposition (3DF) method was used in this study. In addition, the degradation of the amorphous copolymer during the fabrication was studied.

METHODS: Poly(L-lactide-co-ε-caprolactone) was synthesized by ring-opening polymerization with 25 mol% of ε-caprolactone. Both 3DF and solvent casting salt leaching methods were used and compared. In 3DF method, two fabricated patterns (0/90 and 0/45) were created by changing layer angles. An 11-layer-design was used to achieve the thickness of 5mm. The degree of degradation was evaluated by measuring molecular weight at different time points during the fabrication. All the scaffolds were characterized by compression and tensile test for mechanical properties. Human osteoblast-like cells (HOBs) were seeded in scaffolds and cultured under a dynamic environment for 1 and 7 days. The cell distribution and proliferation were studied and evaluated by fluorescence microscopy and scanning electron microscopy.

RESULTS: The degradation of 3DF scaffold during the deposition process was studied and the molecular weight decreased up to 50 % in 6 hours without changing of glass transition temperature. The tensile and compression test of 3DF scaffolds were found to express higher stiffness than the salt leaching scaffolds. With compression to 20% of

original thickness, the scaffolds could almost recover to original size after force release. The cell culture results showed good cell proliferation on

all the samples. However, concentrated HOBs were distributed on the top surface of salt-leached scaffolds. Meanwhile, a homogeneous distribution of cells in 3DF scaffolds was observed on both two patterns of 3DF scaffolds (Fig 1).

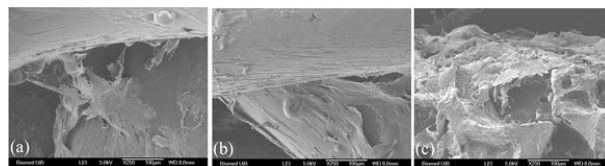


Fig 1: SEM images of scaffolds after 7 days dynamic culturing: 0/90 3DF scaffold (a), 0/45 3DF scaffold (b), and salt leaching scaffold cultured (c). The magnification was set to $\times 250$.

DISCUSSION & CONCLUSIONS: According to the degradation results, the degradation did not affect the glass transition temperature of the material. So it's possible to control the final properties of 3DF scaffolds during the production. Promising data of 3DF scaffolds showed its advantages on mechanical properties and cell distributions. Meanwhile, improved mechanical properties were achieved on 3DF scaffolds comparing with salt-leached scaffolds. The highly organized and reproducible porous structure of 3DF scaffold could support efficient cell nutrition transport. In this study, we have found a solution to produce elastic, degradation controlled, highly interconnected porous reproducible scaffolds using 3DF method for bone tissue engineering use.

REFERENCES: ¹Dänmark, S., Finne-Wistrand, A., Wendel, et al (2010) *Journal of Bioactive and Compatible Polymers* 25(2), 207. ²Idris, S. B., Dänmark, S., Wistrand, A. F., et al (2010) *Journal of Bioactive and Compatible Polymers* vol. 25 no. 6 567-583. ³Sun, Y., Finne-Wistrand, A., Albertsson, A.-C., et al *J. Biomed. Mater. Res. Part A*, 2012; 100(10), 2739-2749.

Effects of load on normal human osteoblast function

A Sundaresan¹, JE Reseland²

¹Texas Southern University, Houston, TX, USA, ²Department of Biomaterials, Institute of Clinical Dentistry, University of Oslo, Norway

INTRODUCTION: Regulation of bone mass is a complex process, involving many factors. It has earlier been proposed that mechanical load influences bone cells, and can enhance formation of bone mass. In this study we wanted to see which effect load has on osteoblasts, and whether different endocrine factors can influence these cells when applied alone or in combination with mechanical loading.

METHODS: Normal Human Osteoblasts (NHOs) (Cambrex) were studied in both undifferentiated states and after 10 days of differentiation. Cells were loaded at 6G, 22G and 50G for 30 min, and compared to cells incubated at 1G. Cell culture medium was harvested 24 and 72 h after loading of the cells and LDH activity, ALP activity, and the levels of OPG, osteocalcin (OC), CD44, leptin, resistin and IL-6 were measured. mRNA was isolated and the expression level of the ALP, OC and leptin measured. In a separate set of experiments, NHOs were seeded on cytodex 3 beads (Sigma) or without and transferred to a NASA rotating wall vessel (modeled microgravity) and cultured for 7-14 days thereafter for a total of 21 days. Constructs were harvested at day 7 and day 14. Frozen sections were stained for ALP and OC. The staining was compared to that of 1g cultures at the same time points.

RESULTS: Results indicated that the load applied had no cytotoxic effect on the cells. Our findings suggest that in undifferentiated cells there is an increase in bone markers (ALP, OC) (Fig. 1) when a moderate load for 30 min is applied, while the secretion of factors known to affect surrounding cells (IL-6, OPG, leptin) (data not shown) slightly decrease with increasing load.

In analog microgravity, there were no changes in the expression of OC and ALP at day 7, but there was a slight decrease in OC day 14 ($p < 0.05$).

Preliminary results in the *in vivo* model of analog microgravity (hind limb unloaded mouse [HU]-1-2 weeks, tail suspension), there is a significant deterioration of bone mass and structure in one week of HU.

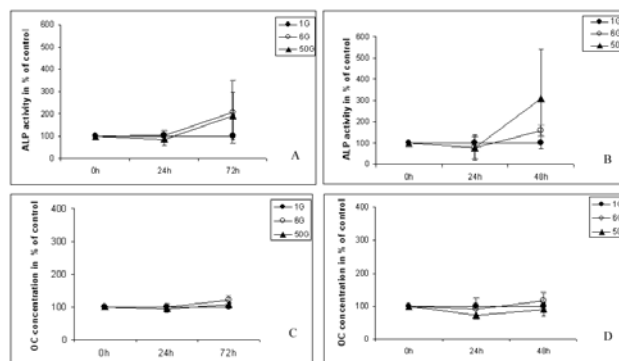


Fig. 1. Effect of loading (● 1G, ○ 6G, ▲ 50G) on ALP activity and OC levels in medium from undifferentiated cells (A and C, respectively) and cells differentiated for 10 days (B and D, respectively). Amount in untreated cells at 1G is set to be 100% at each timepoint.

Bone porosity and connectivity is adversely altered as compared to normal young animals and closer to a two year old mouse. This yields anecdotal evidence of differential osteoblast differential in response to unloading (HU) and possible increased osteoclastogenesis. Fig. 2 shows significant deterioration of bone mass and structure in one week of HU in compared to normal young mice of the same age in 1g (normal).



CONCLUSIONS: Collectively these results demonstrate that load has a differential effect on osteoblast differentiation as seen in modeled microgravity and shows specificity in expression of bone cell markers vs. secreted paracrine signaling markers.

ACKNOWLEDGEMENTS: We wish to thank Drs. Anil Kulkarni, Catherine Ambrose (UT Medical School, Houston) and Koji Wakame (Amino Up, Japan) for their assistance with the “*in vivo*” model and bone histomorphometry.

Highly porous ceramic titanium dioxide scaffolds for bone repair

H Tiainen¹, D Wiedmer^{1,2}, JC Wohlfahrt¹, SP Lyngstadaas¹, HJ Haugen¹

¹*Department of Biomaterials, Institute for Clinical Dentistry, University of Oslo, Norway*

²*Institute of Medical and Polymer Engineering, Chair of Mechanical Engineering, Technische Universität München, Germany*

INTRODUCTION: Synthetic bone scaffolds can be used in assisting the repair and regeneration of bone tissue in critical size bone defects. In this study, the objective was to fabricate highly biocompatible ceramic titanium dioxide (TiO₂) scaffolds with pore architectural and mechanical properties suitable for inducing bone formation from the surrounding tissue in the restoration of large bone defects.

METHODS: Highly porous TiO₂ foams were produced using polymer sponge replication as previously described [1]. SEM imaging and micro-CT analysis were used to examine the pore architectural features of the scaffolds, while the mechanical properties were assessed by compression test. For an *in vivo* animal study, 15 scaffolds were implanted in fresh, surgically treated extraction sockets in minipig mandibles. Bone ingrowth and biocompatibility were evaluated using micro-CT and histology six weeks after implantation.

RESULTS: The produced TiO₂ scaffolds were highly porous (> 85 %) with well-interconnected (> 90% through connections smaller than 250 μm) pore network and mean pore size of ~400 μm (Fig.1), while the average compressive strength of the scaffolds exceeded 3 MPa.

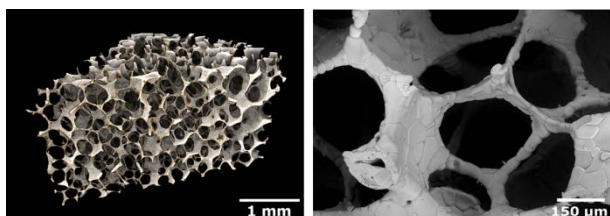


Fig. 1: Typical appearance of the interconnected pore structure of the ceramic TiO₂ scaffolds.

After six weeks of healing, newly formed well-vascularised bone tissue was found to occupy 74 ± 11% of the available pore space within the scaffold structure, and together the scaffold material and regenerated bone filled 84 ± 10% of the total defect volume (Fig.2). In addition, mineralised bone tissue was found in direct apposition with 50 ± 22 % of the TiO₂ struts.

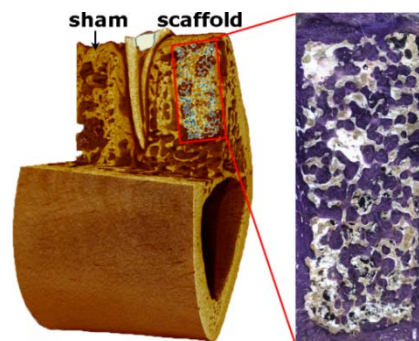


Fig. 2: 3D illustration of the defect sites after six weeks of healing and histological image showing the newly formed bone trabeculae within the scaffold structure.

DISCUSSION & CONCLUSIONS: The produced TiO₂ foams were found to exhibit pore architectural features that closely resemble the structural morphology of highly porous human trabecular bone tissue, and which are well-matched with those required from a bone scaffold, namely high porosity, appropriate pore size distribution, and well-interconnected pore volume. When combined with the excellent biocompatibility of the ceramic TiO₂, the highly interconnected pore structure also provided a favourable micro-environment for bone formation, which was manifested by the ingrowth of large quantity of viable mineralised bone tissue within the porous TiO₂ scaffold structure *in vivo*. As one of the most important prerequisite for a bone scaffold structure is the sufficient permeability of the pore network, the excellent osteoconductive capacity of the TiO₂ scaffolds was attributed to the highly interconnected pore network that allows maximal volume for vascularisation and tissue ingrowth, while still facilitating sufficient structural support at the bone defect site.

REFERENCES: ¹ H. Tiainen, S.P. Lyngstadaas, J.E. Ellingsen et al (2010) *J Mater Sci: Mater Med* **21**:2783-2792.

ACKNOWLEDGEMENTS: This study was supported by Eureka-Eurostars Project Application E!5069 NewBone.

Functional, amorphous and degradable polymers aimed for tissue engineering synthesized by free radical ring-opening polymerization

J Undin¹, A Finne-Wistrand¹, A-C Albertsson¹

¹ *Department of Fibre and Polymer Technology, School of Chemical Science and Engineering, KTH Royal Institute of Technology, Stockholm*

INTRODUCTION: The demand for new materials with controllable and tuneable properties is increasing. Free radical ring-opening polymerization (ROP) is an interesting method since the available cyclic monomers offer attractive ways to design new types of functional polyesters. These monomers, the cyclic ketene acetals are rings with exo-methylene functionalities where the polymerization proceeds by either ring-opening, to form an ester, or ring-retained vinyl addition¹, Fig. 1. Therefore, radical ROP of cyclic ketene acetals can introduce ester groups into the backbone of common vinyl polymers.

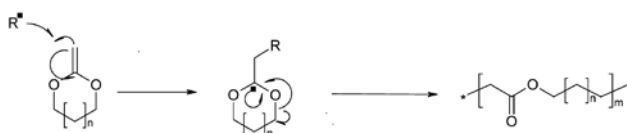


Fig. 1. General reaction of radical ROP of cyclic ketene acetals.

METHODS: The two cyclic ketene acetals, 2-methylene-1,3-dioxepane (MDO) and 2-methylene-1,3,6-trioxocane (MTC), were synthesized in a two step procedure, using a previously described method.^{2,3} The copolymerizations, Fig. 2, were performed in bulk by using 2 mol% of the radical initiator 2,2-azoisobutyronitrile (AIBN) under inert conditions.

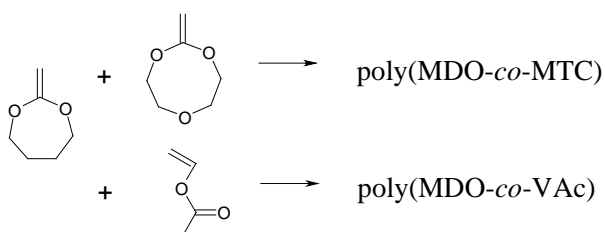


Fig. 2. Copolymerization of MDO with MTC and VAc.

RESULTS: We made two different copolymers to demonstrate some of the numerous design possibilities of the cyclic ketene acetals. First by copolymerization of, MDO and MTC³ to incorporate hydrophilicity into a hydrophobic polymer. Secondly, by copolymerization of MDO with vinyl acetate (VAc)⁴, to add degradability. The monomer feed ratios in the copolymerizations

were varied to understand how the composition, molecular weight (M_n) and glass transition temperature (T_g) can be varied. The results showed that it was possible to control the properties of the final polymers by varying the monomer feed ratios. Some selected results are shown in Table 1.

Table 1. Summary of the copolymerizations

	f_{MDO}	F_{MDO}	M_n (g/mol)	T_g (°C)
MTC	0.75	0.72	2200	-55.1
MTC	0.5	0.44	8600	-54.2
VAc	0.70	0.66	28,300	-50.1
VAc	0.5	0.42	43,700	-45.2

The characteristic of the polyesters made by this route differs from the polyester made by conventional ROP, since branches will occur as a result from hydrogen transfer reactions. These branches decrease the crystallinity and results in amorphous polyesters. The amorphous character of the polyesters is a central parameter and is used as a tool when the degradation is optimized.

DISCUSSION & CONCLUSIONS: The use of cyclic ketene acetals for radical ROP introduces new ways to incorporate functional groups into the polymeric backbone. Radical ROP have many design possibilities and are appealing for further exploration in the tissue engineering field, where tailored, personalized and amorphous properties, and consequently, degradation are important.

REFERENCES: ¹ Bailey, W. J.; Ni, Z.; Wu, S. R. (1982) *J. Polym. Sci., Part A: Polym. Chem.* **20**, 3021. ²Bailey, W. J.; Zhou, L. L. (1991) *Tetrahedron lett.* **32**, 1539. ³Undin, J.; Pliikk, P.; Finne-Wistrand, A.; Albertsson, A.-C. (2010) *J. Polym. Sci., Part A: Polym. Chem.* **48**, 4965. ⁴Undin, J.; Illanes, T.; Finne-Wistrand, A.; Albertsson, A.-C. (2012) *Polym. Chem.* **3**, 1260

ACKNOWLEDGEMENTS: The authors acknowledge ERC Advanced Grant, PARADIGM (grant no: 246776) for their financial support.

simvastatin bound to grit blasted and acid etched titanium zirconium by anodic oxidation increased alkaline phosphatase, collagen type I and osteocalcin expression in vitro

M.S. Walter^{1,3}, M.J. Frank^{1,3}, M. Rubert², M. Monjo², S.P. Lyngstadaas¹, H.J. Haugen¹

¹Department of Biomaterials, Institute for Clinical Dentistry, University of Oslo, Norway. ²Department of Fundamental Biology and Health Sciences, Research Institute on Health Sciences (IUNICS), University of Balearic Islands, Spain. ³Institute of Medical and Polymer Engineering, Chair of Medical Engineering, Technische Universität München, Germany.

INTRODUCTION: Since the discovery of statins' effect on bone growth, research has been conducted with the aim of employing its beneficial properties for therapeutic bone regrowth. This study aims at the application of simvastatin (SVS) on dental implants for use in low density bone. Coin shaped titanium zirconium (TiZr) samples with grit blasted and acid etched (SBAE) surface were coated with simvastatin (SVS) in an anodic oxidation setup under alkaline conditions.

METHODS: The methods for analysis of attachment and integrity of SVS on the coin surfaces were fourier transformed infrared spectroscopy (FTIR), X-ray photoelectron spectroscopy (XPS), secondary ion mass spectroscopy (SIMS), UV visible spectroscopy (UV-VIS). For assessment of topographical and morphological surface changes, field emission SEM (FE-SEM), optical profilometer, and optical microscope were used. An in vitro study using MC3T3-E1 cells was performed to evaluate the cytotoxicity and gene expression of osteoblast markers after cell culture on SVS coated and grit blasted and acid etched titanium zirconium surfaces

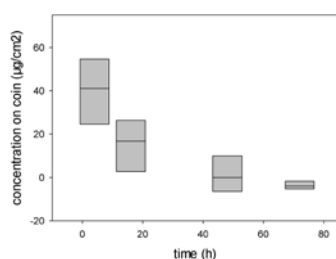


Fig. 1: Release of SVS coated coins over 72 hours in 60 % acetonitrile and 3 % trifluoroacetic-acid mixture (ACN-TFA)

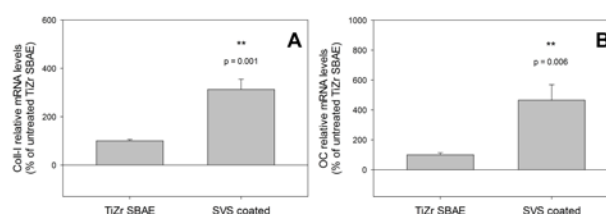


Fig. 2: (A) collagen type I (Coll-I) and (B) osteocalcin (OC) mRNA expression after 14 days. Paired t-test was used for statistical analysis.

DISCUSSION & CONCLUSIONS: The study successfully proved the binding of SVS to a TiZr SBAE surface by means of anodic oxidation. The FTIR analysis found SVS intact on the surface and a method of binding the aliphatic O-H to Ti^{4+} was suggested. This method of binding was furthermore supported by the XPS analysis showing an increased amount of OH-groups on the SVS coated samples. Integration of SVS in the sample surface was documented by the SIMS analysis, showing increased 1H , ^{18}O and ^{12}C isotopes. The release of the molecule over 72 hours showed a SVS concentration of nearly $60 \mu\text{g}/\text{cm}^2$ on the surfaces. Effective release under harsh conditions was detected up to 48 hours after start of the experiment, suggesting a slow release under physiological conditions. The coating of the surface was furthermore demonstrated by high resolution FE-SEM images. The SVS on the sample surfaces was available for the osteoblastic cells and positively influenced their differentiation.

ACKNOWLEDGEMENTS: This work was supported by the Norwegian Research Council (Grants No. 203036). The coin samples were kindly provided by Institut Straumann AG, Basel, Switzerland.

Drug eluting hydroxyapatite coatings for biomedical applications

M Lilja^{1,3}, J Sörensen², U Brohede³, M Åstrand³, P Procter⁴, J Arnoldt⁴, H Steckel², M Strømme^{1*}

¹Division for Nanotechnology and Functional Materials, The Ångström Laboratory, Uppsala University, Box 534, 751 21 Uppsala, Sweden ²Department of Pharmaceutics and Biopharmaceutics, Christian-Albrechts University, 24118 Kiel, Germany, ³Sandvik Coromant Sverige AB, Lerkrogsvägen 19, 12680 Stockholm, Sweden, ⁴Stryker Osteosynthesis AG, 2545 Selzach, Switzerland

INTRODUCTION: Bacterial infection at the site of implanted medical devices presents a challenging problem. Functional implant coatings offering a local release of an antibiotic agent at the infected site are considered to be promising for inhibiting bacterial adhesion and hence for preventing post-surgical infections. While bioactive ceramics and ceramic coatings show promising properties as drug delivery vehicles for transport and sustained release of antibiotics, the longest antibacterial effect demonstrated to date does not exceed three days [1].

METHODS: Stainless Steel fixation pins (Ø 4 mm, 90 mm x 30 mm) were coated with an anatase phase dominated crystalline TiO₂ coating by cathodic arc evaporation [2]. A Hydroxyapatite (HA) coating was biomimetically deposited (HAB) on the TiO₂ coated pins using Dulbecco's PBS. Plasma sprayed HA (HAP) coated fixation pins served as reference substrates. The HA coatings were examined using Scanning electron microscopy (SEM) and X-ray diffraction (XRD). Tobramycin (Sigma) was selected as antibiotic agent and incorporated into the HA coatings by adsorptive loading. The loading and release properties were evaluated by studying the subsequent release of Tobramycin using high pressure liquid chromatography (HPLC) and correlated to the differences in HA coating microstructure and the physical conditions under loading.

RESULTS: The HA coating deposition method had a strong impact on the HA-coating morphology. Whereas plasma spraying resulted in rough HAP morphology, consisting of droplets and variation in substrate coverage, Fig. 1a, HAB coatings showed a nanoporous, continuous coating with needle-like HA crystals, Fig 1b.

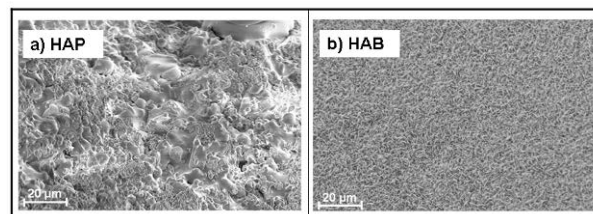


Fig. 1: SEM images of the HAP (a) and the HA-B (b) surfaces

The antibiotic release studied by HPLC showed that during the entire release period the amounts of Tobramycin released from all sample types was above the minimal inhibitory concentration (MIC) for *Staphylococcus aureus*. Both HA coating types showed an initial, burst-like, release within the first minutes of the studied release period. Plasma sprayed coatings released most of the antibiotic during burst, while HAB coatings showed a continuous, and steadily decreasing, release of Tobramycin. The nanoporous structure allowed the antibiotic to penetrate into the structure, resulting in a release period substantially exceeding the three day benchmark.

CONCLUSIONS:

Tobramycin was successfully incorporated into plasma sprayed and biomimetically deposited HA coatings by an adsorptive loading procedure. While the much denser plasma sprayed coatings exhibited only a burst release, a prolonged sustained release was observed during the release from the nanoporous HA coatings obtained through biomimetic deposition. HA coating porosity, coating thickness and drug loading conditions are elemental parameters that can be used to optimize and tailor drug loading capabilities and capacity.

REFERENCES: ¹F. Chai, J.C. Hornez, N. Blanchemain, et al. *Biomol. Eng.* **2007**, *24*, 510. ²M. Lilja, K. Welch, M. Åstrand, et al. (2012) *J. Biomed. Mater. Res. B* 100:1078.